Accepted Manuscript

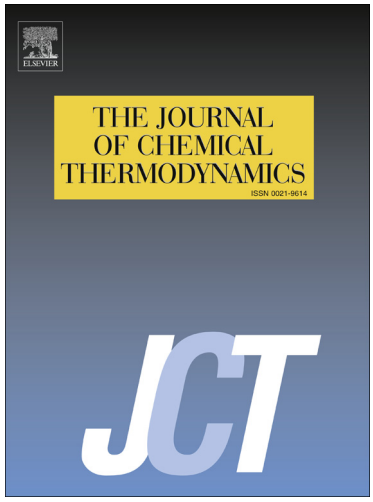

Transport and thermal properties of quaternary phosphonium ionic liquids and IoNanofluids

A.G.M. Ferreira, P.N. Simões, A.F. Ferreira, M.A. Fonseca, M.S.A. Oliveira, A. Trino

PII: S0021-9614(13)00138-9
DOI: http://dx.doi.org/10.1016/j.jct.2013.04.013
Reference: YJCHT 3509

To appear in: *J. Chem. Thermodynamics*

Received Date: 22 February 2013
Revised Date: 15 April 2013
Accepted Date: 16 April 2013

Please cite this article as: A.G.M. Ferreira, P.N. Simões, A.F. Ferreira, M.A. Fonseca, M.S.A. Oliveira, A. Trino, Transport and thermal properties of quaternary phosphonium ionic liquids and IoNanofluids, *J. Chem. Thermodynamics* (2013), doi: http://dx.doi.org/10.1016/j.jct.2013.04.013

This is a PDF file of an unedited manuscript that has been accepted for publication. As a service to our customers we are providing this early version of the manuscript. The manuscript will undergo copyediting, typesetting, and review of the resulting proof before it is published in its final form. Please note that during the production process errors may be discovered which could affect the content, and all legal disclaimers that apply to the journal pertain.

ACCEPTED MANUSCRIPT

Transport and thermal properties of quaternary phosphonium ionic liquids and IoNanofluids

A. G. M. Ferreira [1,*], P. N. Simões[1], A. F. Ferreira[1], M. A. Fonseca[2], M. S. A. Oliveira[2], A. Trino[1]

[1]*Department of Chemical Engineering, University of Coimbra, Polo II, Rua Silvio Lima, 3030-970 Coimbra, Portugal*

[2]*Mechanical Engineering Department, University of Aveiro, Campus Universitário de Santiago, 3810-193 Aveiro, Portugal*

ACCEPTED MANUSCRIPT

[*] Corresponding author at: Department of Chemical Engineering, University of Coimbra, Polo II, Rua Silvio Lima, 3030-970 Coimbra, Portugal.
Tel.: +351 239 798 729; fax: +351 239 798 703.
E-mail address: abel@eq.uc.pt (A. G. M. Ferreira)

ACCEPTED MANUSCRIPT

Abstract

The transport and thermal properties of phosphonium ionic liquids (ILs) and thermally stable suspensions of phosphonium ILs and multiwalled carbon nanotubes (MWCNT) were determined. The thermal conductivity was measured over the temperature range T = (280 to 360) K, and at atmospheric pressure, using the transient hot-wire method with an accuracy estimated as 5 % from (0.2 – 2) $W \cdot m^{-1}K^{-1}$ and less than ± 0.01 $W \cdot m^{-1}K^{-1}$ from (0.02 – 0.2) $W \cdot m^{-1}K^{-1}$. The phosphonium ILs studied were trihexyltetradecylphosphonium phosphinate $[(C_6)_3PC_{14})][Phosph]$, tretrabutylmethylphosphonium methylsulfate, $[(C_4)_3PC_1)][C_1SO_4]$, bis(trifluoromethylsulfonyl)imide, $[(C_6)_3PC_{14}][NTf_2]$, and trihexyltetradecylphosphonium trispentafluoroethyltrifluorophosphate $[(C_6)_3PC_{14}][FAP]$. For all ILs studied, the thermal conductivities were found to lie within the range (0.12 to 0.16) $W \cdot m^{-1} \cdot K^{-1}$. Our measurements combined with selected values from the open literature allowed us to determine a linear increase of combined properties (thermal conductivity, density and molar mass) with the increasing of molar mass. The addition of only (0.1 to 0.2) wt % of MWCNT to ILs (IoNanofluids) revealed a slight increasing of the thermal conductivity from 0.5 % to 1 %. There was also observed a slight decrease of the thermal conductivity with increasing temperature for the ILs alone and respective IoNanofluids. The rheological behaviour of $[(C_6)_3PC_{14})][Phosph]$, of $[(C_6)_3PC_{14})][Phosph]$ and of $[(C_6)_3PC_{14}][NTf_2]$ based IoNanofluids was evaluated at T = (298.15 to 333.15) K and for shear rates in the range $\dot{\gamma}$ = (3 to 30) s^{-1}. All the samples showed shear thinning behaviour. The thermal stability of the IoNanofluids compared to that of ILs alone was studied by High Resolution Thermogravimetric Analysis. It was found that pure $[(C_6)_3PC_{14})][Phosph]$ is a thermally stable IL, whose thermal decomposition under the conditions of this study (2 $K \cdot min^{-1}$) and starts above T = 513 K. It exhibits an one step thermogravimetric profile ($[(C_6)_3PC_{14}][NTf_2]$ that was already investigated in a previous study). A small shift towards lower temperatures was observed in the thermogravimetric curves of IoNanofluids compared to those of the respective ILs alone indicating comparable thermal stabilities. The heat capacities determined by Modulated Differential Scanning Calorimetry within a temperature interval ranging from *ca*. 310 K to 515 K with an estimated uncertainty of less than ±0.012 $J \cdot K^{-1} \cdot g^{-1}$.

Keywords: Ionic liquids; Multi-walled carbon nanotubes; Rheology; Thermal conductivity; Thermal stability; Heat capacity; Predictive models.

ACCEPTED MANUSCRIPT

1. Introduction

The great potential of ionic liquids (ILs) for different kinds of applications has been extensively reported [1,2]. Although thermophysical properties, including transport properties, of ILs have been studied extensively, the data on thermal conductivity available in the open literature is very limited. Currently, a total of 292 data points are available for 34 ILs at atmospheric pressure. The most studied ILs are the alkylimidazolium (or $[C_nC_1im]$) with the bis(trifluoromethylsulphonyl)imide or $[NTf_2]$ anion [3,4]. Experimental determinations of thermal conductivity for the quaternary phosphonium ILs tetrahexyltetradecylphosphonium chloride, $[(C_6)_3PC_{14}][Cl]$, and tetrahexyltetradecylphosphonium bis(trifluoromethylsulphonyl)imide, $[(C_6)_3PC_{14}][NTf_2]$, were made by Ge *et al.* [4] and Gardas *et al.* [5] for several amino acid based ILs with tetrabutylphosphonium $[(C_4)_4P]$ and tributylmethylammonium $[(C_4)_3NC_1]$ cations. Fröba *et al.* [3] have made determinations for trioctylmethylammonium bis(trifluoromethylsulphonyl)imide $[(C_8)_3NC_1][NTf_2]$. As in other properties, the results for thermal conductivity obtained from different laboratories or different methods do not agree within their stated uncertainties due to problems related to the applied methodology or to the purity of the samples. Deviations of about 5 % to 10 % are obtained between different authors.

Given the very large number of ILs, the experimental measurement of the thermophysical properties is not straightforward due to the substantial investment in time and resources that would be necessary. Alternatively, the availability of predictive models based on experimental data, from which the properties of desired accuracy could be obtained, is desirable. Among all transport properties, thermal conductivity is particularly difficult to estimate by predictive methods. Some have been developed for ILs with reasonable accuracy but of limited application over the broad range of different families of ILs. Gardas *et al.* [6] proposed a group contribution model which accounts for the weak dependence of thermal conductivity on temperature. Other authors worked using other basis including the molar mass [3,7]. The use of different families of ILs and the accuracy of the experimental measurements are crucial towards a reliable applicability and utility of predictive methods. Our study aims to provide reliable data for the thermal conductivity of phosphonium ILs covering a broad range of molar mass and different structures, both for the anion and cation. Our results extend the data measured by Ge *et al.* [4] and by Gardas *et al.* [5] for phosphonium-based ILs. The experimental values obtained in this study together with other data selected from the literature provide a predictive method for the thermal conductivity of ILs.

The ability of ILs to disperse and chemically modify CNTs has raised great interest because the resulting suspensions are expected to be stable and homogeneous, leading to (CNT+IL) hybrids with exceptional properties and potential use in a wide range of applications fields [8]. Therefore, another purpose of the present work was the measurement of transport and thermal properties of stable suspensions made of quaternary phosphonium ILs (base fluids) and multi-walled carbon nanotubes (MWCNT). A very good discussion of the impact and importance of these new materials (IoNanofluids) is given by Castro *et al.* [9]. Important enhancements in thermal conductivity and heat capacity are expected because MWCNTs have thermal conductivities at room temperature several orders of magnitude higher than the base fluids. Some studies indicate that a pronounced effect is observed when carbon nanotubes are used for the preparation of nanofluids. Choi *et al.* [10] studied the thermal conductivity enhancement of synthetic poly (α-olefin) oil containing MWCNT with a mean diameter of *ca*. 25 nm and length of *ca*. 50 μm. Measurements were performed at room temperature, and an enhancement of 160 % was observed for 1 v/v % MWCNT/oil nanofluid. The authors noted that such remarkable enhancement might be due to the liquid nanolayers forming around the nanotubes. The fact that heat is transported by a ballistic mechanism inside the nanotubes improves the

ACCEPTED MANUSCRIPT

conduction of heat, but this factor was considered by the same authors as not dominant. For IoNanofluids formed by 1-butyl-3-methylimidazolium trifluoromethanesulphonate ($[C_4C_1im][CF_3SO_3]$) with 1wt % MWCNT, Castro *et al.*[9] obtained enhancements of 9 % on thermal conductivity and observed a weak dependence of this property on temperature.

Viscosity is another relevant transport property needed in many practical applications of ILs that include the formulation of stable electrolytes, lubrication, and solar cells. Their application is however precluded by their high viscosity. A novel method to reduce the viscosity of ILs consists in the addition of small amounts of MWCNTs. Wang *et al.* [11] have studied the rheological behaviour of 1-butyl-3-methylimidazolium hexafluorophosphate ($[C_4C_1im][PF_6]$) with functionalized MWCNTs (F-MWCNTs). These IoNanofluids show shear thinning behaviour at low concentrations of F-MWCNTs (up to 0.1 wt %) which was explained by the high specific size ratio and flexibility of F-MWCNTs and the formation of transient network through CNT-CNT and CNT-liquid matrix interactions. The shear viscosity of these IoNanofluids was lower than that of pure IL especially for high shear rates, and this behaviour was attributed to some self-lubrication of F-MWCNTs. Another important study was made by Neo and Ouyang [12] who were able to reduce the viscosity of 1-propyl-3-methylimidazolium iodide with carboxylic group F-MWCNTs. The viscosity of the IL decreased from 1380 mPa·s to 400 MPa·s at T = 298.15 K after a load of 0.1 wt % of the F-MWCNTs. This study also showed that the blends of MWCNTs with the IL only decrease the viscosity of the IL with loadings up to 0.1 %, and that above this concentration the viscosity raised abruptly to about four times that of the pure IL.

Castro *et al.* [9] have measured the temperature dependence of heat capacity of IoNanofluids made by 1-butyl-3-methylimidazolium hexafluorophosphate (or $[C_4C_1im][PF_6]$) with (1 to 1.5) wt % MWCNT. The results show a dome shaped enhancement with an abrupt maximum of about 8 % which is independent of the CNT loading. The thermal behaviour of IoNanofluids is explained in part by the existence of additional mechanisms of heat transfer related to the formation of nanoclusters and preferred paths for heat transfer and storage.

In our study, we used $[(C_6)_3PC_{14})][Phosph]$ and $[(C_6)_3PC_{14}][NTf_2]$ as base fluids and MWCNTs as nano-additives to fabricate IoNanofluids suspensions with small loadings of carbon nanotubes. The measured properties include the thermal conductivity, viscosity and we have also made thermal studies which include phase transitions and heat capacity measurements determined by Modulated Differential Scanning Calorimetry (MDSC). The thermal stability of the ILs and respective IoNanofluids was studied by High Resolution Modulated Thermogravimetric Analysis (HRMTGA). Recently, we have published experimental values heat capacity of quaternary phosphonium ILs [13].

2. Experimental

2.1 Materials

The $[(C_6)_3PC_{14})][Phosph]$, $[(C_4)_3PC_1)][C_1SO_4]$, and $[(C_6)_3PC_{14}][NTf_2]$, samples were kindly sent upon request by Cytec, under the brand names CYPHOS IL 104, CYPHOS IL 108 and CYPHOS IL 109, respectively. According to Cytec the purity levels are as follows: for $[(C_6)_3PC_{14}][Phosph]$, (CAS # 465527-58-6) typically assay 95 % with the main impurity being tris-2,4,4-trimethylpentyl phosphine oxide, 0.2 to 0.5% of water (by Karl Fisher), and it will contain up to 0.1% of chlorine ion; for $[(C_4)_3PC_1)][C_1SO_4]$, (CAS#34217-64-6) typically assays 98.6 % based on Phosphorus ^{31}P NMR, and a total halide content of 52 ppm. The $[(C_6)_3PC_{14}][NTf_2]$ typically assays 98.6 % based on Phosphorus ^{31}P NMR, and a total halide content of 3 ppm. The $[(C_6)_3PC_{14}][FAP]$ was obtained from Merck (CAS # 883860-35-3) and assays 99.4 % (NMR), < 1% of water (by Karl Fisher), and <0.1 % of halides. The

ACCEPTED MANUSCRIPT

ILs samples were first washed several times using suitable solvents to ensure the removal of any remaining starting materials and next to reduce the water content and volatile species to negligible values a vacuum of about 1 Pa and moderate temperature (343 K) were applied to the IL samples for several days prior to use. The water contents in the dried ILs, determined with a Karl-Fisher 701 KF Titrino coulometer were less than 200 ppm for $[(C_6)_3PC_{14})][Phosph]$, $[(C_4)_3PC_1)][C_1SO_4]$, and $[(C_6)_3PC_{14}][NTf_2]$, and less than 130 ppm for $[(C_6)_3PC_{14}][FAP]$. As will be explained latter, the study of the thermal stability of $[(C_6)_3PC_{14})][Phosph]$ involved a further treatment, consisting in a heating of the washed sample up to 493 K. Table 1 resumes relevant information on sample material purities.
The raw multiwalled carbon nanotubes (MWCNT) were purchased to Shenzehen Nanotech Port Co. Ltd, with the following specifications: outer diameter of (50-80) nm; length of 10-20 μm; ash < 1.5 wt% ; purity > 95 %, specific surface area of 60 $m^2 \cdot g^{-1}$; bulk density: 0.18 $g \cdot cm^{-3}$, and true density of ~2.1 $g \cdot cm^{-3}$. The raw MWCNT were chemically treated, through Esumi *et al.* [14] procedure, in order to ensure a uniform distribution of the MWCNT into the IL. Following this procedure the CNTs are added to a solution of H_2SO_4 and HNO_3 in a proportion of (3:1) and the resulting suspension are mixed in a magnetic stirrer for 30 min at 140ºC. The MWCNTs are then washed with distilled water till a pH~7 is obtained and finally dried in an oven at 100ºC. The treated MWCNT were added to IL and mixed by a magnetic stirrer for 10-20 minutes for a homogeneous distribution. The suspensions of MWCNT in ILs prepared were: $[(C_6)_3PC_{14})][Phosph]$ + MWCNT with a volume fraction of ϕ=0.05% (0.1 % by mass), and $[(C_6)_3PC_{14}][NTf_2]$+ MWCNT with ϕ=0.05% and ϕ=0.1 % (0.1 % and 0.2% by mass).

2.2 Experimental procedure

The thermal conductivity was measured using a KD2 Pro (Decagon Devices). The measurement principle was based on the hot-wire method. The sensing probe was 1.3 mm diameter and 60 mm long, with an accuracy of 5% from 0.2 – 2 $W \cdot m^{-1} \cdot K^{-1}$ and ± 0.01 $W \cdot m^{-1} \cdot K^{-1}$ from 0.02 –0.2 $W \cdot m^{-1} \cdot K^{-1}$. The sensing probe containing a heating element and a thermoresistor was inserted vertically into the sample to minimize the possibility of inducing convection. A volume of sample of ~20 ml was inserted in a double jacketed bottled. Through the use of this double jacketed bottled it was possible to control the sample temperature by the use of a circulating thermal bath. The measurement was made by heating the probe within the sample while simultaneously monitoring the temperature change of the probe. A microcontroller, connected to the probe, was used to control the heating rate, measure the temperature change data, and calculate the thermal conductivity based on a parameter-corrected version of the temperature model given by Carslaw and Jaeger for an infinite line heat source with constant heat output and zero mass, in an infinite medium. The thermal conductivity was measured for temperatures ranging from 283 to 353 K. At least 10 measurements separated by 15 min were taken at each temperature.

Viscosity measurements were carried out using a controlled stress rheometer (Haake model RS1). The rheological tests were made with a Rotor PP20 Titan sensor and using the ThermoHaake heating system. Steady shear measurements were performed in the shear rate range $\dot{\gamma} = (0 \text{ to } 30)\ s^{-1}$, and for temperatures in the range T=(298.15 to 333.15)K. The uncertainty in the measured temperature was ± 0.01K.

The thermal stability of the IoNanofluids ILs was studied by HRMTGA using a TA Instruments Q500 thermogravimetric analyzer (thermobalance sensitivity: 0.1μg). A dynamic rate mode was used under a (maximum) heating rate of 2 $K \cdot min^{-1}$, a modulation period of 200 s, and a temperature amplitude of ± 5 K. The temperature calibration was performed in the range 298-873 ºC by measuring the Curie point of nickel standard, and using open platinum crucibles and a dry nitrogen purge flow of

ACCEPTED MANUSCRIPT

100 mL min^{-1}. This procedure was performed at the heating rate used throughout the experimental work (2 $K \cdot min^{-1}$).

Heat capacity measurements were performed in modulated differential scanning calorimetry (MDSC) equipment from TA Instruments (Q100 model). The heat flow and heat capacity were calibrated at 2 $K \cdot min^{-1}$ using, respectively, indium and sapphire standards. A modulation period of 120~s, and a temperature amplitude of ± 0.53 K were employed. A dry nitrogen purge flow of 50 mL min^{-1} was applied in the calibration and measurements. It should be mentioned that great care was taken to avoid the contact of the sample with moisture during transportation. The room temperature and relative humidity were tightly controlled. The samples were analyzed in aluminium pans with an ordinary pressed aluminium lid, in which a small hole (*ca.* < 0.5mm) was made. The samples were submitted to program in the TGA apparatus before the DSC measurements to ensure the elimination of possible traces of moisture. The procedure consisted in heating the set pan/lid/sample up to 393 K, an isothermal for 5 min, and an equilibration at 298 K. The sample mass observed at this stage was then used as input in the subsequent MDSC run for measuring the heat capacity.

3. Results and discussion

3.1 Thermal conductivity

The experimental thermal conductivities of $[(C_6)_3PC_{14})][Phosph]$, $[(C_4)_3PC_1)][C_1SO_4]$, $[(C_6)_3PC_{14}][NTf_2]$, and $[(C_6)_3PC_{14}][FAP]$ are listed in table 2 and shown in figure 1 compared with other families of ILs. The values of the thermal conductivity of the $[(C_6)_3PC_{14})]$ based ILs ranges from (0.12 to 0.16) $W \cdot m^{-1} \cdot K^{-1}$. The temperature dependence of the thermal conductivity is small, exhibiting a slight decrease with increasing temperature (figure 1), a trend which is similar for all the ILs. The thermal conductivity follows the order: $[(C_6)_3PC_{14}][FAP] < [(C_6)_3PC_{14}][Phosph] < [(C_6)_3PC_{14}][NTf_2] < [(C_4)_3PC_1][C_1SO_4]$. This order and the chemical structure of the respective ILs indicate that the effect of the alkyl chain lengths in the phosphonium cation might have some influence on the thermal conductivity.

For $[(C_6)_3PC_{14}][NTf_2]$, the thermal conductivities measured in our laboratory are systematically lower (about 0.007 $W \cdot m^{-1} \cdot K^{-1}$, corresponding to ≈ 5 %) than those reported by Ge *et al.* [4] using an analogous experimental technique. This difference can be related with the presence of water in the IL, which may alter the thermal conductivity. Some authors studied the influence of water content in thermal conductivity, and they observed an increasing of the thermal conductivity with water content. Ge *et al.* [4] reported a water content of 800×10^{-6} in the $[(C_6)_3PC_{14}][NTf_2]$ samples. This is appreciably more than the water found in our samples, but this difference should not explain by itself the difference in thermal conductivity. Ge *et al.* [4] showed that for imidazolium ILs the addition of small amounts of water, up to a mass fraction of 0.01, had no significant effect on the IL thermal conductivity and that above this mass fraction, the thermal conductivity of the mixture increases always less than the mass fraction average of the thermal conductivities of the pure components. It is interesting to observe in figure 1 a similar effect for 1-butyl-1-methylpyrrolidinium bis(trifluoromethylsulfonyl)imide, (or $[C_4C_1Pyr][NTf_2]$) where the data from Castro *et al.* [8] deviate from those due to Ge *et al.* [4] by 0.007 $W \cdot m^{-1} \cdot K^{-1}$, the before mentioned difference for $[(C_6)_3PC_{14}][NTf_2]$. The water content given by Castro *et al.* [9] is 200×10^{-6} which is similar to that found in our study. Also interesting is the observed behaviour of the thermal conductivity of the quaternary ammonium IL methyltrioctylammonium bis(trifluoromethylsulfonyl)imide, (or $[(C_8)_3NC_1)][NTf_2]$), which is close to the behaviour shown by the quaternary phosphonium $[(C_6)_3PC_{14})][FAP]$. From figure 1, it is observed that the [FAP] anion tends to lower the thermal conductivity: comparing the values for $[(C_6)_3PC_{14})][NTf_2]$ and $[(C_6)_3PC_{14})][FAP]$ for one side, and $[C_4C_1Pyr][NTf_2]$ and $[C_4C_1Pyr][FAP]$ for the other, the same decrease of 0.012 $W \cdot m^{-1} \cdot K^{-1}$ (about 10 %) is observed. The slight decrease of the thermal conductivity with increasing temperature observed in ILs may be correlated with convection effects that are not so

ACCEPTED MANUSCRIPT

significant in such materials. The thermal conductivity, k, of each IL studied as a function of the temperature, T, was fitted with a linear equation

$$k = k_0 + k_1 T \quad (1)$$

where k_0 and k_1 are the fitting parameters whose values and respective uncertainties (standard deviation) given in table 3.

The thermal conductivity data obtained for the IoNanofluids resulting from the addition of MWCNTs to the $[(C_6)_3PC_{14})][Phosph]$ and $[(C_6)_3PC_{14}][NTf_2]$ ILs were measured over the temperature range from 280 K to 353 K and are presented in table 2 and in figure 2. It can be seen that the variation with temperature is almost linear, as for the pure phosphonium ILs. There is also present some constancy with temperature at higher values of this property, and that the addition of MWCNTs to the ILs results in a slight increase in thermal conductivity. The thermal conductivity enhancement can be defined in percentage as $100(k_{NF}/k_B - 1)$ where k_{NF} and k_B are, respectively, the thermal conductivity of the IoNanofluid and the base fluid (IL). Moderate enhancements in the thermal conductivity were observed for the IoNanofluids: 0.4 % to 1.4 % for $[(C_6)_3PC_{14})][Phos]$+MWCNT (ϕ = 0.05 %) and 0.5 % for $[(C_6)_3PC_{14})][NTf_2]$+MWCNT (ϕ = 0.1 %). These results are close to those obtained by Castro *et al.* [9] for the system $[C_6C_1im][PF_6]$+MWCNT with a mass percent of 1 % MWCNTs, which is much greater than the mass fractions used in our study (0.1 to 0.2) %. Those authors obtained the following enhancements on thermal conductivity: $[C_6C_1im][BF_4]$, (3 to 7) %; $[C_4C_1im][CF_3SO_3]$, (8 to 10) %; $[C_4C_1Pyr][NTf_2]$, (5 %); $[C_4C_1im][PF_6]$ (2 to 3) %; and $[C_6C_1im][PF_6]$ (1 to 2) %. It should be noted that the volumetric fractions of the IoNanofluids studied by Castro *et al.* [9] were in the range ϕ = (6 to 7)%, which corresponds to 70 to 140 times higher than the values used in our work. Therefore, we conclude that phosphonium Ionic Liquids are suitable base fluids to be used in thermal conductivity enhancement with MWCNTs.

The prediction of thermal conductivity of ILs is very important for the reasons mentioned above. The predictive methods are scarce but some pioneer work has been devoted to this issue. Tomida *et al.* [7] and Fröba *et al.* [3] tried to connect thermal conductivity with the molecular structure, while Gardas and Coutinho [6] developed a group contribution method with the same purpose. Fröba *et al.*[3] found for $[NTf_2]$-based ILs a small increase of the thermal conductivity with increasing molar mass of the cation at a given temperature, probably due to internal vibration modes which are important for the heat conduction in addition to the translation modes. For $[C_2C_1im]$-based ILs a pronounced, an approximately linear, decrease with increasing molar mass of the anions was observed. This could be explained by a decreasing effect of these vibration modes with the increase of the molecular size of the anion. In figure 3, it is shown the behaviour of the thermal conductivity, k, as a function of the molar mass, M, of the phosphonium ILs studied in this work and of some other ILs selected from the literature at T = 298.15 K and atmospheric pressure. It is interesting to observe that k decreases almost linearly with the molar mass for all the quaternary $[(C_6)_3PC_{14})]$ ILs. This is probably due to the complex interactions between ions which determine a decreasing effect of the vibration/translation modes as the molecular size of the anion increases. Considering the size limits, the chloride ion is small with an effective volume of 27 $cm^3 \cdot mol^{-1}$ [15], while the [FAP] anion has an effective volume of 226 $cm^3 \cdot mol^{-1}$ [15], apart from the more elaborated structure and complex Coulombic and dispersion forces. The data corresponding to $[NTf_2]$ anion, taken from Fröba *et al.*[3] and Ge *et al.* [4], follow a linear increasing tendency despite the differences in the measured data by the two authors: Ge *et al.* [4] always obtained greater values of thermal conductivity than Fröba *et al* [3] by (0.005 to 0.007) $W \cdot m^{-1} \cdot K^{-1}$. The almost linear increasing trend of thermal conductivity as a function of the molar mass for $[NTf_2]$ anion is verified for different cations either cyclic as the imidazolium ($[C_nC_1im]$, $2<n<10$, $[C_4C_4im]$), pyrrolidinium, $[C_4C_1Pyr]$, or for the quaternary

ACCEPTED MANUSCRIPT

ammonium, [$(C_8)_3NC_1$] and phosphonium, [$(C_6)_3PC_{14}$)]. The data for [$(C_8)_3NC_1$][NTf_2] has a particular linear consistency with all the data measured by Fröba *et al.*[3] and our value for [$(C_6)_3PC_{14}$][NTf_2].

Fröba *et al.* [3] combined values of thermal conductivity, density and molar mass by plotting the group ($k\rho M$) as a function of the molar mass M for [C_2C_1im] and for [NTf_2] based ILs at T = 293.15 K. Curiously, they obtained a single common linear trend, suggesting that the thermal conductivity of the studied ILs at the above mentioned temperature can be predicted from

$$k\,\rho\,M = A + BM \tag{2}$$

where A= 22.065 $g^2 \cdot cm^{-3} \cdot W \cdot m^{-1} \cdot K^{-1}$ and B=0.1130 $g \cdot cm^{-3} \cdot W \cdot m^{-1} \cdot K^{-1}$. Furthermore, taking into account all the experimental data for the thermal conductivity up to that time, Fröba *et al.* [3] proposed the universal correlation (at T= 293.15 K):

$$k\,\rho\,M = 18.84 + 0.1244\,M \tag{3}$$

From equation (3), a mean absolute percentage deviation of 6.5 % between the experimental and the predicted values was obtained for 45 data points from a set of 36 ILs. In figure 4, we represent ($k\rho M$) as a function of M for the phosphonium ILs studied in this work and also other ILs, at T=298.15 K and atmospheric pressure. The density and thermal conductivity of all the ILs at T=298.15 K, respectively ρ_{298} and k_{298}, are listed in table 4. The densities at T = 298.15 K were obtained for some ILs from the equation

$$ln\,\rho = \rho_0 + \rho_1\,T + \rho_2\,T^2 \tag{4}$$

where ρ_0, ρ_1 and ρ_2 were obtained by fitting selected experimental density data for the several ILs taken from the references also given in table 4. The thermal conductivities of ILs of this work and from other sources at the same temperature were obtained from equation (1). In figure 4, it can be seen that the ILs with ring cations (alkylimidazolium and pyrrolidinium) define a separate trend when compared to the linear quaternary ammonium and phosphonium ILs, and that the tendencies are somewhat independent of the anions. Therefore we propose two linear equations:

$$(k\,\rho\,M) = (18.464 \pm 2.190) + (0.134 \pm 0.006)\,M \tag{5}$$

$$(k\,\rho\,M) = (8.533 \pm 1.999) + (0.136 \pm 0.004)\,M \tag{6}$$

for ring cations and for linear quaternary alkyl ILs, respectively. The standard deviations for the fittings are σ (ring) = 3.90 $g^2 \cdot cm^{-3} \cdot W \cdot m^{-1} \cdot K^{-1}$ and σ (quaternary) = 2.99 $g^2 \cdot cm^{-3} \cdot W \cdot m^{-1} \cdot K^{-1}$. Table 4 and figure 4 show that the linear correlation given by equation (5) can be applied over the ranges M = (170 to 590) $g \cdot mol^{-1}$ of molar mass, and k = (0.11 to 0.21) $W \cdot m^{-1} \cdot K^{-1}$ of thermal conductivity for ring structured cations. On the other hand, equation (6) is applicable for the ranges M = (300 to 930) $g \cdot mol^{-1}$ of molar mass and k = (0.11 to 0.21) $W \cdot m^{-1} \cdot K^{-1}$ of thermal conductivity for quaternary ammonium and phosphonium cations. It can be seen that [$(C_6)_3PC_{14}$)][Phosph] deviates considerably from the linear tendency. This can be due to the combined low thermal conductivity and density but the most likely factor can be the impurity tris-2,4,4 trimethylpentyl phosphine oxide which was *ca*. 5 % by weight. This substance has a boiling point of T = 746.55 K and cannot be eliminated by the washing and vacuum purification procedure described earlier above (see also section 3.3). The results for the other phosphonium ILs are in good agreement with the observed trend. In figure 4, the data are also represented equation (3) established by Fröba *et al.*[3] at T=293.15 K because k decreases very slowly

ACCEPTED MANUSCRIPT

with temperature and therefore a difference from T = 298.15 K will be not significant. It can be observed that equation (3) proposed by Fröba *et al.* describes an intermediate behaviour between the two equations found for ring and linear quaternary cations, but cannot describe accurately the behaviour of quaternary phosphonium and ammonium ILs, at least at low molar mass. However, the differences are not significant and equation (3) describes in a semi-quantitative way all the observed tendencies. Figure 5 shows quite good agreement of the predicted thermal conductivity, k_{calc}, with the corresponding experimental values, k_{exp}, for the ILs reported so far, combined with those studied in this work at T= 298.15 K and atmospheric pressure. For the 52 ILs considered, only five of them present calculated values of thermal conductivity with deviations higher than 10 %. The values of the thermal conductivity of $[C_2C_1im][BF_4]$ observed by Valkenburg *et al.* [1], and that of $[C_6C_1im][BF_4]$ measured by Castro *et al.* [9] deviate by 12 % and 14% respectively. However for $[C_4C_1im][BF_4]$, the predicted and experimental values from different authors are in accordance. For $[C_4C_1im][PF_6]$ the experimental value from Frez *et al.*[43] deviates by 35 % from the value calculated through the equation (5). However the calculated value is in accordance with the determinations from Tomida *et al.* [7]. The value of thermal conductivity of $[C_4C_1im][NTf_2]$ given by Frez *et al.* [47] at T = 298.15 K deviates by about 15 % from the value calculated from equation (5), but these values are in agreement (relative deviation of 3 %) with the one reported by Ge *et al.* [4]. Frez *et al.* [47] did not indicate the contaminants (and purity of studied ILs) but described a careful preparation and purification by washing with water and drying under vacuum. Those authors also referred that the NMR spectra were in excellent agreement with the expected characteristics of each component of ILs, and that the method used in the measurement of thermal conductivity was the transient grating method which gives uncertainties of the order of 4 %. The $[(C_6)_3PC_{14})][Phosph]$ IL deviates by 23 % from the calculated value. Removing the five points responsible for relative deviations higher than 10 % from the whole tested set, the average absolute relative deviation is of 4 %.

An important aspect of the research on heat transfer in nanofluids is the prediction of the thermal conductivity enhancement. More than a century ago, after the Maxwell equation for calculating the effective thermal conductivity of solid-liquid mixtures consisting of spherical particles [48], several models have been proposed. Some mechanisms have been suggested so far to explain the anomalous thermal conductivity enhancement of nanofluids. The most important are: (i) the Brownian motion, *i.e.* the random motion of particles suspended in a fluid; (ii) the clustering of nanoparticles which can result in fast transport of heat along relatively large distances as explained by Evans *et al.* [49]; (iii) the liquid layering around nanoparticles [50,51]; (iv) the ballistic phonon transport in nanoparticles, although the studies made by Keblinski *et al.* [52] show that this effect is important for nanofluids with very small nanoparticles, which is not the case of the IoNanofluids with MWCNT; (v) the near field radiation effect that can take place when the distance between the nanoparticles is smaller than the diameter of the particles [53]. Some studies have shown that the near field interactions between nanoparticles do not significantly affect the thermal conductivity of the nanofluid [54]. Castro *et al.* [9] pointed out that the major mechanisms responsible for the enhancement of thermal conductivity in nanofluids are the effect of surface chemistry and the structure of the interface particle/fluid. Xie *et al.* [55] studied the effect of the interfacial nanolayer on the enhancement of thermal conductivity with nanofluids. A nanolayer was modelled as a spherical shell with thickness t around the nanoparticle. The nanolayer thermal conductivity was assumed to change linearly across the radial direction, so that it is equal to thermal conductivity of the base liquid at the nanolayer–liquid interface and equal to thermal conductivity of the nanoparticle at the nanolayer–nanoparticle interface. The prediction of the thermal conductivity of nanofluid following Xie *et al.* [55] is made by the following equations

$$\frac{k_{NF} - k_{IL}}{k_{IL}} = 3\Theta\phi_T + \frac{3\Theta^2\phi_T^2}{1-\Theta\phi_T} \qquad (7)$$

ACCEPTED MANUSCRIPT

where k_{NF} and k_{IL} are the thermal conductivities of nanofluid and base fluid (IL), respectively, and

$$\Theta = \frac{\beta_{I/IL}\left[(1+\gamma)^3 - \frac{\beta_{pl}}{\beta_{IL/1}}\right]}{(1+\gamma)^3 + 2\beta_{1/IL}\beta_{pl}} \quad , \tag{8}$$

where subscripts IL, l, p refer respectively to the IL (base fluid), the nanolayer and to the particle (CNTs), and

$$\beta_{l/IL} = \frac{k_l - k_{IL}}{k_l + 2k_{IL}} \; , \; \beta_{p/l} = \frac{k_p - k_l}{k_p + 2k_l} \; , \; \beta_{IL/l} = \frac{k_{IL} - k_l}{k_{IL} + 2k_l} \tag{9}$$

where k_l and k_p are the thermal conductivities of nanolayer and particle, respectively. The total volume fraction of nanoparticles and nanolayers ϕ_T is

$$\phi_T = \phi(1+\gamma)^3 \tag{10}$$

where $\gamma = t/r_p$ and r_p is the radius of nanoparticles. k_l is defined as

$$k_l = \frac{k_{IL}M^2}{(M-\gamma)\ln(1+M) + \gamma M} \tag{11}$$

where

$$M = \varepsilon_p(1+\gamma) - 1 \; , \; \varepsilon_p = k_p / k_{IL} \tag{12}$$

The studies regarding why and how the liquid layers are formed are very limited. There is also a lack of detailed examination of properties of these layers, such as their thermal conductivity and thickness. Since ordered crystalline solids have normally much higher thermal conductivity than liquids, the thermal conductivity of such liquid layers is believed to be higher than that of bulk liquid. The thickness t of such liquid layers around the solid surface can be estimated by [56] the following equation,

$$t = \frac{1}{\sqrt{3}}\left(\frac{4M_{IL}}{\rho_{IL}N_A}\right)^{1/3} \tag{13}$$

Hwang *et al.* [57] considered values of about k_p =3000 $W \cdot m^{-1} \cdot K^{-1}$ for MWCNT with outer diameter of (10-30) nm and length of (10-50) μm while Choi *et al.*[58] refer values of k_p= 2000 $W \cdot m^{-1} \cdot K^{-1}$. Therefore we considered the range k_p= (2000 – 3000) $W \cdot m^{-1} \cdot K^{-1}$ of thermal conductivity for the MWCNTs. When equation (13) is applied to $[(C_6)_3PC_{14}][NTf_2]$ IoNanofluids at T = 298.15 K gives t =1 nm which is a value comparable to $t \approx 2$ nm suggested by Choi *et al.* [58]. Following Murshed *et al.* [59], the value of this parameter is not critical for the calculations. For r_p = (25 - 40) nm and taking k_p in the range mentioned before, equation (7) gives enhancements of nearly 0.3 % and 0.4 % when t =1 nm and t =2 nm, respectively. The values of enhancements are about one half than those experimentally obtained and therefore we conclude that this model represents qualitatively the

ACCEPTED MANUSCRIPT

experimental results in the range of studied volumetric fractions. If t ≈ 10 nm is used we obtain enhancements of 0.6 % to 0.8%, which are of the same magnitude of the experimental values of this work. The value predicted for k_l is of the order of 190 $W \cdot m^{-1} \cdot K^{-1}$ when $t \approx 1$ to 2 nm but rises up to 300 $W \cdot m^{-1} \cdot K^{-1}$ for I ≈ 10 nm. These values are higher than the proposed ($k_l = 60\ k_{IL}$) made by Murshed *et al.* [59] for ethylene glycol/CNTs nanofluids.

3.2 Viscosity

The viscosity is related to the internal resistance of a fluid to a shear stress and the rheological measurements can provide useful information about the microstructure of fluids. The rheological data which include the shear rate, $\dot{\gamma}$, and the viscosity, η, are given for several temperatures as supporting information in table S1. The flow curves (η, $\dot{\gamma}$) of the prepared IoNanofluids are shown in figures 6 and 7. From figure 6, it can be clearly seen that the shear (or apparent) viscosity decreases dramatically at first, then gradually, to a stable value beyond $\dot{\gamma} = 30\ s^{-1}$ shear rate and this behaviour is particularly evident at 323.15 K and 333.15 K. These results show a typical non-Newtonian, shear thinning (or pseudo-plastic) flow behaviour being [$(C_6)_3PC_{14}$)][Phosph] a typical example. This behaviour can be due to the aggregates existing in the liquid phase that can be disrupted or broken at higher shear rates leading to smaller values of the viscosity. Increasing the temperature, the shear thinning is shifted to lower shear rates indicating that a smaller or less cohesive aggregate has been in action, and at higher temperature a Newtonian behaviour is approximated at lower shear rates. Since viscosity is mainly dependent on intermolecular interactions (H-bonding, dispersive and Coulombic interactions) an increase of temperature weakens such interactions and lowers the viscosity. To date researchers have treated pure ILs as Newtonian fluids because the instrumentation used in the measurement of this property is suitable only for Newtonian behaviour. No research effort has been specifically directed towards investigation of potential non-Newtonian behaviour of ILs. However, some few studies indicate a shear thinning for imidazolium based ILs. Wang *et al.* [60] studied a new class of IL crystals (ILCs) based on 1,3-didodecylimidazolium salts ([$C_{12}C_{12}$im]), showing thermotropic liquid crystalline behaviour in an extended temperature range below 343 K. Remarkably strong non-Newtonian viscosity behaviour was found for the liquid-crystalline state of these ILCs. These authors reported that for [$C_{12}C_{12}$im][BF_4] a pronounced shear thinning at liquid crystalline temperatures T = (338.15, 343.15) K was observed but the Newtonian behaviour was found at T = (353.15, 363.15) K. Other examples of non-Newtonian behaviour are provided by [C_3C_1im][I] [12] and [C_4C_1im][PF_6] [11]. This behaviour was verified also in diisopropyl-ethylammonium-based protic ILs [61]. From figure 6, we can conclude that the addition of a small amount of MWCNTs (≈ 0.1 wt % corresponding to $\phi = 0.05$ %) can remarkably reduce the viscosity of [$(C_6)_3PC_{14}$)][Phosph]. At (T= 298.15 K, $\dot{\gamma} = 30\ s^{-1}$) shear thinning is observed with apparent viscosity of 1990 mPa·s but for the IoNanofluid at the same conditions of temperature and shear rate the viscosity is η=350 mPa·s. The corresponding reduction in drag index as defined by Phuoc *et al.* [62]

$$D_{index} = 100\left(\frac{\tau_{NF} - \tau_b}{\tau_b}\right) \tag{14}$$

where τ_{NF} and τ_b are the shear stress of IoNanofluids and of the base fluid(IL) is D_{index}= 82 %. It is interesting to observe a tendency to equilibrium which corresponds to almost constant values of viscosity of the IoNanofluids at higher temperatures: at T = (313.15, 323.15) K the viscosity of IoNanofluids is always lower than that of the pure IL ($\eta \approx 200$ mPa·s at $\dot{\gamma} = 30\ s^{-1}$). The IoNanofluids with [$(C_6)_3PC_{14}$)][NTf_2] as base fluid show a markedly thinning behaviour. However, the reduction in the viscosity of the corresponding IoNanofluid is much smaller when compared to that for phosphinate IL, which takes place at higher shear rates at a given temperature, being more evident at lower

ACCEPTED MANUSCRIPT

temperatures. The shear thinning effect of IoNanofluids can be in part explained as before for the $[(C_6)_3PC_{14})][Phosph]$ IL, but now with additional realignment of bundled nanostructures of CNTs in the direction of shearing forces, leading to smaller values of viscous drag. The viscosity change of ILs by loading MWCNTs is certainly due to the interaction between the ions of the ILs and the carbon nanotubes. One can advance the possibility of some kind of functionalization of the CNTs by the IL, *viz.* non-covalent functionalization of CNTs which normally involves van der Waals, π-π, CH- π, or electrostatic interactions between ions and CNT surface. This kind of functionalization is mentioned in polymer-CNTs composites [63]. In some sense, ILs can be physically resembled as polymers. Shear thinning behaviour with reduction of viscosity by loading MWCNTs and F-MWCNTs to the ILs has been reported [11, 12]. As the reduction of the viscosity effect in the $[(C_6)_3PC_{14})][Phosph]$ based IoNanofluid is greater than for the $[(C_6)_3PC_{14})][NTf_2]$ IoNanofluid. One extra factor that can be responsible is the possible interaction between phosphinate anion and the CNT surface, possibly through the group [RPOO-) in the phosphinate anion. This will shield the Coulombic attractions between the cations and the anions resulting in a decrease of viscosity. Other phenomena probably related with the flexibility and mobility of the ions should be also involved, hence resulting in a more complex scenario.

The non-Newtonian, shear thinning behaviour of $[(C_6)_3PC_{14})][Phosph]$ IL and of the IoNanofluids was here described analytically by the modified Quemada model due to the simplicity and good accuracy of model. In this model, the apparent viscosity, η, is defined by the following equation [64]

$$\eta = \left(\eta_\infty^{\,1/2} + \frac{\tau_0^{\,1/2}}{\lambda^{1/2} + \dot{\gamma}^{1/2}} \right) \tag{15}$$

where η_∞, τ_0, and λ are constitutive coefficients. The coefficient η_∞ is the upper shear rate limit for viscosity (or limiting high shear rate Newtonian viscosity). In many cases, this means that after this limit the fluid behaves like a Newtonian fluid and non-Newtonian models should reach the Newtonian viscosity. The parameter λ is a shear rate modifier which prevents the singularity and computation of unreal viscosity when $\dot{\gamma}$ approaches zero and its use increases the accuracy of the model, especially within low shear rate ranges. The parameters η_∞, τ_0, and λ were obtained by fitting equation (15) to the experimental (η, $\dot{\gamma}$) values, and are given in table 5. The experimental data and results of fitting equation (15) are shown in figures (6) and (7). For T = (313.15 and 323.15) K , the upper shear rate limit values of the viscosity for $[(C_6)_3PC_{14})][Phosph]$ IL are near the experimentally measured values by Neves *et al.* [43] (relative deviations of 5 %).

3.3 Thermal stability

To the best of our knowledge, there are no published thermoanalytical results on $[(C_6)_3PC_{14})][Phosph]$, thus being of interest to start this discussion considering this IL. Figure 8 presents the HRMTGA and respective time derivative curves of two samples of $[(C_6)3PC_{14})][Phosph]$. One of such samples was used in the thermoanalytical measurements as received after being washed as described in section 2.1; the other (washed) sample was submitted to a thermal treatment consisting in a 2 $K \cdot min^{-1}$ heating ramp up to T = 493 K, and an isothermal stage at this temperature for 5 min. It can be observed that the sample as received exhibits two mass loss stages within well separated temperature intervals, suggesting two independent steps. The first mass loss of 5.4 % is observed in the approximate temperature range 370 K to 500 K (extrapolated onset temperature, T_{on}, of 429 K). This event should correspond to the loss of the main impurity characterizing the raw sample, *viz.* tris-2,4,4-trimethylpentyl phosphine oxide, whose removal by simple washing seems not to be possible. The

ACCEPTED MANUSCRIPT

actual decomposition of $[(C_6)_3PC_{14})][Phosph]$ in an almost pure state occurs within the temperature range 513 K to 613 K (T_{on} ~ 555 K). In fact, including in the discussion the thermo-analytical results of the preheated sample, it can be observed in figure 8 that the thermal decomposition profile of the IL itself is not affected by the impurity it contains. Above T = 500 K, the thermo-analytical curves of both samples (without and with thermal treatment) are essentially overlapped, as can be checked from some pertinent points obtained from the thermo-analytical curves summarized in table 6. In short, $[(C_6)_3PC_{14})][Phosph]$ is a thermally stable IL, which, under the conditions of this study, start to decompose above T = 513 K and exhibits an one step decomposition thermo-gravimetric profile.

The results in figure 9 and in table 6 show how the suspension of MWCNT in the ILs influences the thermal stability of the latter *per se*. For the $[(C_6)_3PC_{14})][Phosph]$+MWCNT system, a shift by no more than 6 K towards lower temperatures is observed in the HRMTGA curve as a whole, a result that can be interpreted as a modest decrease in the thermal stability. The thermal decomposition of $[(C_6)_3PC_{14}][NTf2]$ as revealed by HRMTGA proceeds through two consecutive steps, possibly more, as suggested by the derivative curve, with some overlapping between them. The very beginning of the decomposition and the immediately following sharp mass loss stage are not influenced by the presence of the MWCNT. Such influence is evident only in the subsequent stages, again by a shift of the thermo-gravimetric curve in the direction of lower temperatures.

3.4 Heat capacity

The heat capacity as function of temperature was measured for $[(C_6)_3PC_{14})][Phosph]$ alone and for the IoNanofluids {$[(C_6)_3PC_{14})][Phosph]$+MWCNT} and {$[(C_6)_3PC_{14})][NTf_2]$+MWCNT}. The experimental values are presented as supporting information in table S2 and displayed in figure 10a. The error bars given correspond to the uncertainty of the experimental data which were found at each temperature from several series of experiments for each fluid/suspension system. The maximum uncertainty of 0.012 $J\cdot K^{-1}\cdot g^{-1}$ was found for $[(C_6)_3PC_{14})][NTf_2]$ and was obtained from heat capacity measurements made by us previously [13]. The heat capacity $[(C_6)_3PC_{14})][Phosph]$ measured in this work shows the higher value at a given temperature in the phosphonium series presented in our previous work [13], and the values increase in the order $[(C_4)_3PC_1][C_1SO_4]$ < $[(C_6)_3PC_{14}][Cl]$ < $[(C_6)_3PC_{14}][DCA]$ < $[(C_6)_3PC_{14}][NTf_2]$ < $[(C_6)_3PC_{14}][FAP]$ < $[(C_6)_3PC_{14})][Phosph]$. It should be noted that the heat capacity was measured for the $[(C_6)_3PC_{14})][Phosph]$ sample that contains tris-2,4,4-trimethylpentyl phosphine oxide as the main impurity and that heat capacity enhancement of $[(C_6)_3PC_{14})][Phosph]$-based IoNanofluid is relative to that sample. However the amount of impurity present presumably cannot significantly alter the values of heat capacity found for the pure IL. From figure 10a, it can be observed that the heat capacity increases significantly with the increase of temperature according to a slightly curved trend. The experimental values are well correlated trough the polynomial expression

$$C_p = c_0 + c_1 T + c_2 T^2 \qquad (16)$$

where c_0, c_1, c_2 are parameters obtained by fitting whose values are presented in table 7 where the standard deviation of the fittings is also given. The heat capacity enhancement, $C_{p(NF)}/C_{p(f)}$ -1, is given as a function of temperature in figure 10b. The enhancement increases slowly for $[(C_6)_3PC_{14})][Phosph]$-based IoNanofluid from 7 % at T = 293.15 K up to 8 % at 363.15 K, but for $[(C_6)_3PC_{14})][NTf_2]$ IoNanofluid the enhancement has an almost constant value of 13 % over the entire temperature range. This difference in heat capacity enhancement can be partly explained by the higher load in CNTs for the $[(C_6)_3PC_{14})][NTf_2]$ IoNanofluid (≈ 0.2 wt % compared with ≈ 0.1 wt % for $[(C_6)_3PC_{14})][Phosph]$). Our results are different from those found by Castro *et al.* [9] for $[C_4C_1im)][PF_6]$+MWCNT IoNanofluids. These authors observed that regardless of MWCNT loading

ACCEPTED MANUSCRIPT

(1-1.5) wt % there was a dome-shaped jump of the heat capacity enhancement with a peak increasing of 8 % compared to the base IL. This jump occurred within the temperature range 333.15 K to 383.15K. The reasons for this strange behaviour remain not well understood. Nevertheless, the maximum observed enhancement is of comparable magnitude of that measured in this work for $[(C_6)_3PC_{14})][Phosph]$ IoNanofluid, which contained one tenth of the load of that experienced by Castro *et al.* [9]. It is advisable that more work be done with phosphonium ILs to confirm the results found in this work using both lower and higher nano-additive loadings.

Another important study concerning heat capacity of (IL+MWCNT) systems was made by Wang *et al.* [65] whose work reports different results when compared with our results and those from Castro *et al.* [9]. The measurements made by Wang *et al.* [68] for $\{[C_6C_1im)][BF_4]$ + MWCNT$\}$ – dispersed IoNanofluids with nano-additive loading of 0.03 % and 0.06 wt % in the range T = (293.15 to 353.15) K showed that the heat capacity increased with temperature for both pure ILs and IoNanofluids, but the values of the heat capacity of the latter were lower than the neat IL at the same temperature. For the IoNanofluid containing 0.06 wt % of MWCNTs, the decrease in heat capacity was ≈ 2 % over the temperature range studied. A similar behaviour was observed for the same loadings of graphene in $[C_6C_1im)][BF_4]$.

Following Shin and Banerjee [66], the enhancement of heat capacity can be explained by three independent competing intermolecular mechanisms. One of these considers that nanoparticles have higher specific heat capacity individually than when they are in bulk conditions. The surface atoms in the lattice of the nanoparticle are less constrained due to the fewer number of bonds. Therefore the surface atoms vibrate at a lower frequency and higher amplitudes resulting in higher surface energy. The second mechanism involves the solid-fluid interaction energy. The CNT particles have high surface area per unit mass and this cause an anomalous increase in the interfacial thermal resistance between the nanoparticles and surrounding liquid molecules. This high interfacial thermal resistance should act as additional heat storage due to the interfacial interaction of the vibration energies between nanoparticle atoms and the interfacial molecules. The third mechanism is due to a semi-solid layer formation. The liquid molecules adhering on the surface of the CNTs have a semi-solid behaviour and enhance specific heat capacity due to the smaller inter-molecular spacing similar to the nanoparticle lattice structure on the surface (compared to the higher inter-molecular spacing in the bulk liquid). Such a layer of semi-solid molecules would not exist in the absence of the nanoparticles. The thickness of this adhesion layer of liquid molecules would depend on the surface energy of the nanoparticle. These semi-solid layers usually have higher heat capacity than the bulk liquid and therefore contribute to increasing the effective specific heat capacity of nanofluid. Molecular dynamics studies demonstrated the existence of the semi-solid layer surrounding nanoparticles [67]. Also TEM images showed the experimental evidence for ordering of liquid molecules on the interface between liquid molecules and nanoparticles [68]. The molecular dynamics results show that the semi-solid layer of liquid molecules on a crystalline surface is constrained to a region that is 2–5 nm in thickness. According to Shin and Banerjee [66], the number of adhered layers of the liquid molecules is expected to be a function of the surface energy of the crystalline interface. Also for a given mass fraction of the nanoparticles, an optimum size of the nanoparticle can be expected to exist in order to maximize the mass fraction of the adhered molecules from the liquid-phase, forming the semi-solid layer thus providing an optimum in the enhancement of the specific heat capacity of the nanofluid. In addition, the optimum concentration of the nanoparticles can be a function of the nanoparticle nominal size or the size distribution of the nanoparticles.

The equation

$$C_{p(\mathrm{NF})} = \frac{\phi_\mathrm{p}\rho_\mathrm{p}C_{p(\mathrm{p})} + \phi_\mathrm{f}\rho_\mathrm{f}C_{p(\mathrm{f})}}{\phi_\mathrm{p}\rho_\mathrm{p} + \phi_f\rho_f} \tag{17}$$

ACCEPTED MANUSCRIPT

where $C_{p(\mathrm{NF})}$ is effective specific heat capacity of the nanofluid, $C_{p,(\mathrm{f})}$ is specific heat capacity of the base fluid, $C_{p,(\mathrm{p})}$ is specific heat capacity of the particle, ϕ_{p} is volume fraction of the particle, ϕ_{f} is yjr volume fraction of fluid, ρ_{p} is the density of the particle, and ρ_{f} is the density of fluid, is not suitable to describe the behaviour of (IL+ MWCNT) IoNanofluids referred in this section. Equation (17) was developed by Xuan and Roetzel [69] under the assumption of local thermal equilibrium between the nanoparticles and the base fluid. Vajjha and Das [70] developed the following general specific heat correlation

$$\frac{C_{p(\mathrm{NF})}}{C_{p,(\mathrm{f})}} = \frac{AT + B\left(\dfrac{C_{p(\mathrm{p})}}{C_{p(\mathrm{f})}}\right)}{(C + \phi_{\mathrm{p}})} \tag{18}$$

where A, B, and C area fitting parameters. It is interesting to observe that the term $(C_{p(\mathrm{NF})}/C_{p(\mathrm{f})})$ can be taken as a measure of the heat capacity enhancement. As calculations show for the $[(C_6)_3PC_{14})][\mathrm{Phosph}]$ IoNanofluid the term $(C_{p(\mathrm{p})}/C_{p(\mathrm{f})}) = (0.355\pm0.006)$ is almost independent of the temperature in the temperature range of the measurements. For this system: A= 2.188x10^{-4}, B= 2.898, C= 1.031, σ=±0.001. For the $[(C_6)_3PC_{14})][NTf_2]$ IoNanofluid, the term $(C_{p(\mathrm{NF})}/C_{p,(\mathrm{f})}) = (1.129\pm0.002)$ but the ratio $(C_{p,(\mathrm{p})}/C_{p(\mathrm{f})})$ increases non-linearly with the temperature and thus equation (18) cannot accurately describe the observed behaviour. The failure of the equations (17) and (18) when applied to (IL+ MWCNT) IoNanofluids is certainly due to the simple and empirical assumptions which do not incorporate the action of the complex mechanisms mentioned before, especially the solid-fluid interaction energy which allows the extra energy storage or the layering effect which was already considered in the development of models for thermal conductivity. The heat capacity of carbon nanotubes has been studied by several research groups. Results are available for single-walled carbon nanotubes (SWCNT) [71,72], double walled (DWCNT) [71] and MWCNT [72-75]. Pradhan *et al.* [72] measured the heat capacity of two different samples of MWCNT in the range T = (300 to 400) K and they have concluded that randomly oriented CNTs, MWCNT(R) show a similar heat capacity behaviour of bulk graphite powder, and that their values were much higher than those for highly ordered and aligned MWCNT(A). This behaviour is presented in figure 10a. Since the heat capacity of MWCNT is less than one half than the IoNanofluids, possibly the first of the three before mentioned mechanisms can be of small importance in the heat capacity enhancement.

4. Conclusions

The values of the thermal conductivity of four quaternary phosphonium ILs were determined over the temperature range T = (280 K to 360) K, and at atmospheric pressure, using the transient hot-wire method with an uncertainty estimated less than ± 0.01 W·m^{-1}K^{-1}. The thermal conductivity, viscosity, thermal stability and heat capacity of thermally stable suspensions of phosphonium ILs and multi-walled carbon nanotubes (IoNannofluids) were determined, over the same temperature range as the ILs *per se*. The thermal conductivity of the ILs and the IoNannofluids shows a weak dependence on temperature. The decrease of the thermal conductivity with the increasing of temperature can be well represented by a linear correlation. Moderate thermal conductivity enhancements of 0.4 % to 1.4% were observed for the IoNannofluids with phosphonium ILs as base fluids. The enhanced thermal conductivity can be considered of relevance when compared to the scarce results from the literature obtained by other authors for other different families of ILs, and working with volume fractions which are one hundred times higher than those used in this study. Therefore, we conclude that phosphonium

ACCEPTED MANUSCRIPT

ILs are very suitable as base fluids to be used in thermal conductivity enhancement and that higher loadings of MWCNTs, possibly higher than 1 wt. %, must be tested in future studies. For the ILs alone, our measurements combined with selected values from the literature allowed to find a linear correlation of the combined properties (thermal conductivity, density and molar mass) with the molar mass. Two correlations were observed, one for the ring and the other for quaternary cations. The combined average absolute relative deviation corresponding to the two correlation equations was 4 %.

The viscosity of $[(C_6)_3PC_{14})][Phosph]$ and the prepared phosphonium-based IoNanofluids show non-Newtonian thinning behaviour over the temperature range studied and with the increase of temperature the shear thinning is shifted to lower shear rates, indicating that smaller or less cohesive aggregates are formed. The viscosity of IoNanofluids is considerably lowered by comparing with the base IL. For $[(C_6)_3PC_{14})][Phosph]$-based IoNanofluid with only 0.05 v/v % (or $\approx$ 0.1wt %) of MWCNT the decrease of viscosity is 82 %. On the other hand, the heat capacity of the IoNanofluids is enhanced up to a maximum value of 13 % for $[(C_6)_3PC_{14})][NTf_2]$-based IoNanofluid. The combination of great viscous drag reduction with heat capacity enhancement makes the (phosphonium + MWCNT) system important and promising IoNanofluids to be used in practical clean-energy related applications, as thermal storage, battery electrolytes, and dye-sensitized solar cells. More studies on viscosity and heat capacity of phosphonium+MWCNT systems must be done to reinforce and to improve the results presented here. It will be convenient to research issues as the higher loadings of MWCNTs and F-MWCNTs.

The thermal stability of the IoNanofluids has been studied by HRMTGA, and the heat capacities determined MDSC within a temperature interval ranging from *ca*. 310 K to 515 K with an estimated uncertainty is less than ± 0.012 $J \cdot K^{-1} \cdot g^{-1}$. The $[(C_6)_3PC_{14})][Phosph]$ behaves as a thermally stable IL, which, under the conditions of this study, exhibits an one step decomposition thermogravimetric profile. The presence of MWCNT in the two ILs studied produces nothing but a modest shift of the thermogravimetric curve towards lower temperatures, meaning that the IoNanofluids studied form thermally stable systems.

ACCEPTED MANUSCRIPT

ACCEPTED MANUSCRIPT

Acknowledgments

The authors acknowledge CYTEC Canada, Inc., Niagara Falls, ON, for supplying PBILs, and in particular to Mr. Jean-Paul Garnier EMEA Sales Manager, CYTEC Industries, France for the fast shipping of phosphonium ILs samples.

The authors acknowledge the support from Dr. M. G. Rasteiro during the rheology tests undertaken in the Chemical Process Engineering and Forest Products Research Centre.

ACCEPTED MANUSCRIPT

ACCEPTED MANUSCRIPT

Appendix A. Supplementary data

Supplementary data associated with this article can be found, in online version at http:...

References

[1] M.E.Van Valkenburg, R.L. Vaughn, M. Williams and J.S. Wilkes, Thermochimica Acta 425 (2005) 181–188.

[2] S. *Aparicio,* M. *Atilhan,* F. Karadas, Ind. Eng. Chem. Res. 49 (2010) 9580-9595.

[3] A. P. Fröba, M. H. Rausch, K. Krzeminski, D. Assenbaum, P. Wasserscheid and A. Leipertz, Int J. Thermophys. 31 (2010) 2059–2077

[4] R. Ge, C. Hardacre, J. Jacquemin, P. Nancarrow, D. W. Rooney, J. Chem. Eng. Data, 27 (2007) 1819-1823.

[5] R. L. Gardas, R. Ge, P. Goodrich, C. Hardacre, A. Hussain, D. W. Rooney, Chem. Eng. Data, 55 (2010) 1505–1515.

[6] R. L. Gardas, J. A. P. Coutinho, AIChE J. 55 (2009) 1274-1290.

[7] D. Tomida, S. Kenmochi, T. Tsukada, K. Qiao, C. Yokoyama, Int. J. Thermophys.28 (2007) 1147-1160.

[8] S. U. S.Choi, J. Heat Transf. Trans. ASME 131(3) (2009) Nº 033106,1-9]

[9] C. A, Nieto de Castro, M. J. V.Lourenço, A. P. C Ribeiro, E. Langa, S. I. Vieira, P. Goodrich, C. Hardacre, J. Chem. Engi. Data, 55 (2010) 653–661.

[10] Choi, S. U. S., Zhang, Z. G., Yu, W., Lockwood, F. E., and Grulke, E. A., 2001, "Anomalous Thermal Conductivity Enhancement in Nanotube Suspensions," Appl. Phys. Lett., **79**(14), pp. 2252-2254.

[11] B. Wang, X. Wang, W. Lou, J. Hao, J. Phys.Chem. C 114 (2010) 8749-8754.

[12] C. Y. Neo, J. Ouyang, Electrochim. Acta 85 (2012) 1-8.

[13] A. F. Ferreira, P. N. Simões, A. G. M. Ferreira, J. Chem. Thermodynamics 45 (2012) 16–27.

[14] K. Esumi, M. Ishigami, A. Nakajima, K. Sawada, H. Honda, Carbon 34 **(1996)** 279-281.

[15] Jacquemin, R. Ge, P. Nancarrow, D. W. Rooney, M. F. Costa Gomes‡, A. A. H. Pádua, C. Hardacre, J. Chem. Eng. Data, 53 (2008) 716-726.

[16] A. Wandschneider, J. K. Lehmann and A. Heintz, J. Chem. Eng.Data, 2008, 53, 596–599.

ACCEPTED MANUSCRIPT

[17] M. Tariq, A. P. Serro, J. L. Mata, B. Saramago, J. M. S. S. Esperança, J. N. C. Lopes and L. P. N. Rebelo, Fluid Phase Equilib., 2010, 294, 131–138.

[18] R. L. Gardas, M.G. Freire, P.J. Carvalho, I.M. Marrucho, I.M.A. Fonseca, A.G.M. Ferreira, J.A.P. Coutinho, J. Chem. Eng. Data *52* (2007) 1881-1888.

[19] N. Tariq, P.A.S. Forte, M. F. Costa Gomes, J. N. Canongia Lopes, L. P. N. Rebelo, J. Chem. Thermodyn. 41 (2009) 790-798.

[20] Q. Zhang, Z. Li, J. Zhang, S. Zhang, L. Zhu, J. Yang, X. Zhang and Y. Deng, J. Phys. Chem. B, 2007, 111, 2864–2872.

[21] M. Deetlefs, K. R. Seddon and M. Shara, Phys. Chem. Chem. Phys., 2006, 8, 642–649.

[22] C. Kolbeck, J. Lehmann, K. R. J. Lovelock, T. Cremer, N. Paape, P. Wasserscheid, A. P. Fro¨ ba, F. Maier and H.-P. Steinru¨ ck, J. Phys. Chem. B, 2010, 114, 17025–17036.

[23] A. Ahosseini, B. Sensenich, L. R. Weatherley and A. M. Scurto, J. Chem. Eng. Data, 2010, 55, 1611–1617.

[24] A. Muhammad, M. I. A. Mutalib, C. D. Wilfred, T. Murugesan and A. Shafeeq, J. Chem. Thermodyn., 2008, 40, 1433–1438.

[25] L. I. N. Tomé, P. J. Carvalho, M. G. Freire, I. M. Marrucho, I. M. A. Fonseca, A. G. M. Ferreira, J. A. P. Coutinho, R. L. Gardas J. Chem. Eng. Data 53 (2008) 1914-1921.

[26] B. Hasse, J. Lehmann, D. Assenbaum, P. Wasserscheid, A. Leipertz and A. P. Fröba, J. Chem. Eng. Data 54 (2009) 2576–2583.

[27] C. P. Fredlake, J.M. Crosthwaite, D.G. Hert, S.N.V.K. Aki, J.F. Brennecke. J. Chem. Eng. Data, 49 *(*2004*)* 954–964.

[28] R. L. Gardas, H. F. Costa, M. G. Freire, P. J. Carvalho, I. M. Marrucho, I. M. A. Fonseca, A. G. M. Ferreira, J. A. P. Coutinho J. Chem. Eng. Data. 53 (2008) 805-911.

[29] M. Shamsipur, A. Akbar, M. Beigi, M. Teymouri, S. M. Pourmortazavi and M. Irandoust, J. Mol. Liq., 157 (2010) 43–50.

[30] L. G. Sánchez, J. R. Espel, F. Onink, G. W. Meindersma and A. B. de Haan, J. Chem. Eng. Data, 54 (2009) 2803–2812.

[31] E. Rilo, J. Pico, S. Garcia-Garabal, L. M. Varela and O. Cabeza, Fluid Phase Equilib.,285 (2009) 285, 83–89.

[32] R. L. Gardas, M. G. Freire, P. J. Carvalho, I. M. Marrucho, I. M. A. Fonseca, A. G. M. Ferreira, J. A. P. Coutinho, .J. Chem. Eng. Data 52 (2007) 80-88.

[33] J. Jacquemin, P. Husson, V. Mayer, and I. Cibulka, J. Chem. Eng. Data 52, (2007) 2204-2211.

[34] Y.A. Sanmamed, D. Gonzalez-Salgado, J. Troncoso, C.A. Cerdeirina, L. Romani,. Fluid Phase Equilib. 252 (2007) 96–102.

[35] P. Navia, J. Troncoso, L. Romanı, J. Chem. Eng. Data 52 (2007) 1369-1374.

[36] G. García-Miaja, J. Troncoso, L. Romaní, J. Chem. Thermodyn. 41, (2009) 334-341

[37] J. Klomfar, M. Součková, J. Pátek, Fluid Phase Equilib. 282, (2009) 31-37.

[38] A. Stoppa, O. Zech, W. Kunz and R. Buchner, J. Chem. Eng. Data 55 (2010) 1768-1773.

[39] Z. Gu, J. F. Brennecke, J. Chem. Eng. Data 47 (2002) 339-345.

[40] J. Klomfar, M. Součková, J. Pátek, J. Chem. Eng. Data 56 (2011) 3454-3462.

ACCEPTED MANUSCRIPT

[41] P. Kilaru, G. A. Baker and P. Scovazzo, J. Chem. Eng. Data 52 (2007) 2306–2314.

[42] F. A. M. M. Gonçalves, C. S. M. F. Costa, C. E. Ferreira, J. S. Bernardo, I. Johnson, I. M. A. Fonseca, A. G. M. Ferreira, J. Chem. Thermodyn. 43 (2011) 914-929.

[43] C.M.S.S. Neves, P.J. Carvalho, M.G. Freire, J.A.P. Coutinho, J. Chem. Thermodyn. 43 (2011) 948–957.

[44] J.M.S.S. Esperança, H.J.R. Guedes, M. Blesic, L.P.N. Rebelo, J. Chem. Eng. Data 51(2006) 237–242.

[45] C. E. Ferreira, N. M.C. Talavera-Prieto, I. M.A. Fonseca, A.T.G. Portugal, A. G.M. Ferreira, J. Chem. Thermodynamics 47 (2012) 183–196.

[46] CYPHOS 108, Cytec Industries, Canada, Niagara Falls, ON.

[47] C. Frez, G. J. Diebold, C. D. tran, S. Yu, J. Chem. Eng. Data, 51 (2006) 1250-1255.

[48] J. C. Maxwell, *A Treatise on Electricity and Magnetism*, Clarendon Press, Oxford, UK, 1873.

[49] W. Evans, R. Prasher, J. Fish, P. Meakin, P. Phelan, P. Keblinski, Int. J. Heat Mass Tran., 51 (2008) 1431-1438.

[50] C. Yu, A. G. Richter, A. Datta, M. K. Durbin, P. Dutta, Phys. Rev. Lett., 82 (1999) 2326-2329.

[51] W. Yu, S. U. S Choi, J. Nanopart. Res., 5 (2003) 167-171.

[52] P. Keblinski, S. R. Phillpot, S. U. S. Choi, J. A. Eastman, Int. J. Heat Mass Tran., 45 (2002) 855-863.

[53] G. Domingues, S. Volz, K. Joulain, J. Greffet, Phys. Rev. Lett., 94 (2005), 085901.

[54] P. Ben-Abdallah, Appl. Phys. Lett., 89 (2006) 113117-3.

[55] H. Xie, M. Fujii, X. Zhang, Int. J. Heat Mass Trans. 48 (2005) 2926-2932.

[56] B. X. Wang, L. P. Zhou, X. F. Peng, Int J Heat Mass Transfer 46 (2003) 2665- 2672 .

[57] Y. Hwang, J. K. Lee, C.H. Lee, Y.M. Jung, S.I. Cheong, C.G. Lee, B.C. Ku, S.P. Jang ,Thermochimica Acta 455 (2007) 70–74.

[58] S. Choi, Z. Zhang, W. Yu, F. Lockwood, E. Grulke, Appl. Phys. Lett. 79 (2001), 2252–2254.

[59] S. Murshed, S. M. S., Leong, K. C. & Yang, C. Int. J. Therm. Sci., 47 (2008) 560-568.

[60] X. Wang, F. W. Heinemann, M. Yang, B. U. Melcher, M. Fekete, A-V. Mudring, P. Wasserscheid, K. Meyer, Chem. Commun. 47 (2009) 7405-7407.

[61] J. Jacquemin, M. Anouti, D. Lemordant, J. Chem. Eng. Data, 56 (2011) 556–564.

[62] T. X. Phuoc, M. Massoudi, R-H. Chen Int. J. Therm. Science 50 (2011) 12-18.

[63] M. T. Byrne, Y. K. Gun'ko, Adv. Mater. 22 (2010) 1672–1688.

[64] J. R. Buchanan Jr., C. Kleinstreuer, J. K. Comer, Computers and Fluids 29 (2000) 695-724.

[65] F. Wang, L. Han, Z. Zhang, X. Fang1, J. Shi,W. Ma, Nan. Res. Let. 7 (2012) 314-320.

[66] D. Shin, D. Banerjee, International Journal of Heat and Mass Transfer 54 (2011) 1064–1070.

[67] L. Li, Y. Zhang, H. Ma, M. Yang, , J. Nanoparticle Res. 12 (2010) 811–821.

[68] S.H. Oh, Y. Kauffmann, C. Scheu, W.D. Kaplan, M. Rühle, Science 310 (2005) 661–663.

[69] Xuan Y, Roetzel W: Conceptions for heat transfer correlation of nanofluids. Int J Heat Mass Transf. 2000, 43:3701-3707.

ACCEPTED MANUSCRIPT

942 [70] R. S. Vajjha, D. K. Das, J. Heat. Transf. 131 (2009) 1-7.

943 [71] G. G. Silva, A. W. Musumeci, A. P. Gomes, J. W. Liu, E. R. Waclawik, G. A. George, R. L.
944 Frost, M. A. Pimenta, Mater Sci (2009) 44:3498–3503.

945 [72] N. R. Pradhan, D. H, Liang J, G. S. Iannacchione , Nanotechnology 20 (2009) 245705.

946 [73] V. B. Muratov, O. O. Vasil'ev, L. M. Kulikov, V. V. Garbuz, Yu. V. Nesterenko, T. I. Duda, J.
947 Sup. Materials, 34 (2012) 173–178.

948 [74] C. Masarapu, L. L.Henry, B. Wei. J. Nanotechnology 16 (2005) 1490-1494.

949 [75] W. Yi, L. Lu, Zhang Dian-lin, Z. W. Pan,S. S. Xie, Phys. Rev. B, 59 (1999) R9015-R9018.

950
951
952
953
954 **Captions for figures**
955
956 FIGURE 1. Thermal conductivity of phosphonium ILs. ▲, $[(C_6)_3PC_{14})][FAP]$; ▼,
957 $[(C_6)_3PC_{14})][Phosph]$; ♦, $[(C_6)_3PC_{14})][NTf_2]$; ◊, $[(C_6)_3PC_{14})][NTf_2]$, Ge *et al.*[4]; ■,
958 $[(C_4)_3PC_1)][C_1SO_4]$; ○$[C_6C_1im][BF_4]$, Castro *et al.*[9]; ★, $[C_4C_1Pyr][NTf_2]$, Castro *et al.*[9]; ☆,
959 $[C_4C_1Pyr][NTf_2]$ Ge *et al.*[4]; +, $[(C_8)_3NC_1)][NTf_2]$ Fröba *et al.*[3]; ×, $[C_4C_1Pyr][FAP]$ Ge *et al.*[4].
960 Solid lines designated equation (1) with parameters given in table 3.
961
962
963 FIGURE 2. Thermal conductivity of the $[(C_6)_3PC_{14})][Phosph]$, and $[(C_6)_3PC_{14}][NTf_2]$ ILs, pure and
964 with MWCNTs. ▼, $[(C_6)_3PC_{14})][Phosph]$; ∇, $[(C_6)_3PC_{14})][Phospho]$ + MWCNT (ϕ=0.05 v/v%); ♦,
965 $[(C_6)_3PC_{14})][NTf_2]$; ◊, $[(C_6)_3PC_{14})][NTf_2]$+ MWCNT (ϕ=0.05 v/v%); ⊕, $[(C_6)_3PC_{14})][NTf_2]$ +
966 MWCNT (ϕ=0.1 v/v%). Lines designated equation (1) with parameters given in table 3.
967 .
968
969 FIGURE 3. Thermal conductivity *k*, for the studied phosphonium and other ILs from the literature at *T*
970 = 298.15 K and atmospheric pressure as a function of the molar mass M. Legend: ▼,
971 $[(C_6)_3PC_{14})][Cl]$, Ge *et al.* [4]; ■, $[(C_6)_3PC_{14}][NTf_2]$; +, $[(C_6)_3PC_{14}][NTf_2]$, Ge *et al.* [4]; ●,
972 $[(C_6)_3PC_{14})][Phosph]$; ▲, $[(C_6)_3PC_{14})][FAP]$; ⛬, $[(C_4)_3PC_1)][C_1SO_4]$; ○, $[C_2C_1im][NTf_2]$, Fröba *et*
973 *al.*[3]; ∇, $[C_4C_1im][NTf_2]$, Ge *et al.* [4];⊛, $[C_6C_1im][NTf_2]$, Fröba *et al.*[3]; ⊞, $[C_6C_1im][NTf_2]$, Ge *et*
974 *al.* [4]; ★, $[C_8C_1im][NTf_2]$, Ge *et al.* [4]; ⌖, $[C_{10}C_1im][NTf_2]$, Ge *et al.* []; ⊕, $[C_4C_4im][NTf_2]$ Fröba
975 *et al.*[3]; ◑, $[C_3C_1C_1im][NTf_2]$ Van Valkenburg *et al.* [1]; Fröba *et al.*[3]; ⛛, $[C_4C_1Pyr][NTf_2]$, Ge
976 *et al.* [4];◓, $[(C_8)_3NC_1][NTf_2]$ Fröba *et al.*[3]; △, $[C_4C_1Pyr][FAP]$, Ge *et al.* [4]; ◊, $[C_2C_1im][BF_4]$,
977 Van Valkenburg *et al.* [1]; ⊕, $[C_4C_1im][BF_4]$, Van Valkenburg *et al.* [1]; ⬗, $[C_4C_1im][PF_6]$; ⬖,
978 $[C_6C_1im][PF_6]$; ⬘, $[C_8C_1im][PF_6]$; ☆, $[C_2C_1im][OAc]$; ⬓, $[C_2C_1im][EtSO_4]$; ⬙, $[C_2C_1im][C(CN)_3]$; ×,
979 $[C_2C_1im][N(CN)_2]$; ⬡, $[(C_4)_3NC_1][Ser]$ Gardas *et al.* [5]; ⌬,$[(C_4)_3NC_1][Tau]$ Gardas *et al.* [5]; ⎔,
980 $[(C_4)_3NC_1][Lys]$ Gardas *et al.* [5]; ⊕, $[(C_4)_3NC_1][Thr]$ Gardas *et al.* [5]; ◐, $[(C_4)_4P][Ser]$ Gardas *et al.*
981 [5]; ◒, $[(C_4)_3NC_1][Tau]$ Gardas *et al.* [5]; ◓, $[(C_4)_3NC_1][Lys]$ Gardas *et al.* [5]; ⛗, $[(C_4)_3NC_1][Thr]$
982 Gardas *et al.* [5]; ⛚, $[(C_4)_3NC_1][Pro]$ Gardas *et al.* [5]; ⛙, $[(C_4)_3NC_1][Cys]$ Gardas *et al.* [5].
983
984 FIGURE 4. Combination ($k\rho M$) as a function of the molecular mass, *M*, for the studied phosphonium
985 and other ILs from literature at *T* = 298.15 K and atmospheric pressure.
986 Legend: ▼, $[(C_6)_3PC_{14})][Cl]$; ■, $[(C_6)_3PC_{14}][NTf_2]$; +, $[(C_6)_3PC_{14}][NTf_2]$; ●, $[(C_6)_3PC_{14})][Phosph]$; ▲,
987 $[(C_6)_3PC_{14})][FAP]$; ⛬, $[(C_4)_3PC_1)][C_1SO_4]$; ○, $[C_2C_1im][NTf_2]$; ∇, $[C_4C_1im][NTf_2]$; ⊛,
988 $[C_6C_1im][NTf_2]$; ⊞, $[C_6C_1im][NTf_2]$; ★, $[C_8C_1im][NTf_2]$; ⌖, $[C_{10}C_1im][NTf_2]$; ⊕, $[C_4C_4im][NTf_2]$;

ACCEPTED MANUSCRIPT

◑, $[C_3C_1C_1im][NTf_2]$; ⛛, $[C_4C_1Pyr][NTf_2]$; ◓, $[(C_8)_3NC_1][NTf_2]$; △, $[C_4C_1Pyr][FAP]$; ◊, $[C_2C_1im][BF_4]$; ⊕, $[C_4C_1im][BF_4]$; ◭, $[C_4C_1im][PF_6]$; ◮, $[C_6C_1im][PF_6]$; ◆, $[C_8C_1im][PF_6]$; ☆, $[C_2C_1im][OAc]$; ◘, $[C_2C_1im][EtSO_4]$; ✥, $[C_2C_1im][C(CN)_3]$; ×, $[C_2C_1im][N(CN)_2]$; ⬡, $[(C_4)_3NC_1][Ser]$; ⬡,$[(C_4)_3NC_1][Tau]$; ⬢, $[(C_4)_3NC_1][Lys]$; ⊕, $[(C_4)_3NC_1][Thr]$; ◐, $[(C_4)_4P][Ser]$; ◒, $[(C_4)_3NC_1][Tau]$; ◔, $[(C_4)_3NC_1][Lys]$; ⛒, $[(C_4)_3NC_1][Thr]$; ◔, $[(C_4)_3NC_1][Pro]$; ⛒, $[(C_4)_3NC_1][Cys]$; (——), linear fitting for cyclic cations; (----), linear fitting for linear quaternary cations; (-·-·-), Fröba *et al.* model, equation (3).

FIGURE 5. Linear relationship between experimental and the predicted thermal conductivity using equations (5) and (6). Legend: ○, Ring cations ILs; Δ, Linear quaternary cations ILs; ILs deviating more than 10 %: ⊕, $[C_4C_1im][NTf_2]$; ●, $[C_4C_1im][PF_6]$; ▲, $[(C_6)_3PC_{14})][Phosph]$; ⊕, $[C_6C_1im][BF_4]$; ◑, $[C_2C_1im][BF_4]$; (----), ± 10 % relative deviation.

FIGURE 6. Apparent viscosity (η) as a function of shear rate ($\dot{\gamma}$) and temperature for $[(C_6)_3PC_{14})][Phosph]$ and IoNanofluids $[(C_6)_3PC_{14})][Phosph]$+0.05 v/v% MWCNTs. Legend: $[(C_6)_3PC_{14})][Phosph]$, ▲, T = 298.15 K; ●, T = 313.15 K; ■, T = 323.15 K; ♦, T = 333.15 K; $[(C_6)_3PC_{14})][Phosph]$+0.05 v/v% MWCNTs, Δ, T = 298.15 K; ○, T = 313.15 K; □, T = 323.15 K. The symbols at $\dot{\gamma}$=100 s^{-1} refer to values given by Neves *et al.* [43] for Newtonian behaviour: ⛬, T=298.15 K; ⊕, T=313.15 K; ⊞, T=323.15 K; ⊕, T=333.15 K. The lines correspond to calculated values with equation (15).

FIGURE 7. Apparent viscosity (η) as a function of shear rate ($\dot{\gamma}$) and temperature for $[(C_6)_3PC_{14})][NTf_2]$+0.1 v/v% MWCNTs IoNanofluids. Legend: Δ, T=298.15 K; ○, T=313.15 K; ◊,, T=333.15 K. The symbols at $\dot{\gamma}$=100 s^{-1} refer to values given by Neves *et al.* [43] for Newtonian behaviour: ⛬, T=298.15 K; ⊕, T=313.15 K; ⊕, T=343.15 K. The lines correspond to calculated values with equation (15).

FIGURE 8. HRMTGA curves (top) and respective time derivatives (bottom) of $[(C_6)_3PC_{14})][Phosph]$ samples (2 °C·min^{-1}; amplitude of modulation: ±5 °C; period of modulation 200 s).

FIGURE 9. HRMTGA curves (top) and respective time derivatives (bottom) of IL samples and their IoNanofluids counterparts (2 °C·min^{-1}; amplitude of modulation: ±5 °C; period of modulation 200 s).

FIGURE 10. (a) Heat capacity (Cp) as a function of the temperature for $[(C_6)_3PC_{14})][Phosph]$ and IoNanofluids. Legend: ■, $[(C_6)_3PC_{14})][Phosph]$, ●, $[(C_6)_3PC_{14})][NTf_2]$, □, $[(C_6)_3PC_{14})][Phosph]$+0.05 v/v% MWCNTs; ○, $[(C_6)_3PC_{14})][NTf_2]$+0.1 v/v% MWCNTs; Δ, MWCNT(A) [72]; ∇, MWCNT(R) [72]. (b) Heat capacity enhancement of IoNanofluids as function of temperature T. □, $[(C_6)_3PC_{14})][Phosph]$+0.05 v/v% MWCNTs; ○, $[(C_6)_3PC_{14})][NTf_2]$+0.1 v/v% MWCNTs.

ACCEPTED MANUSCRIPT

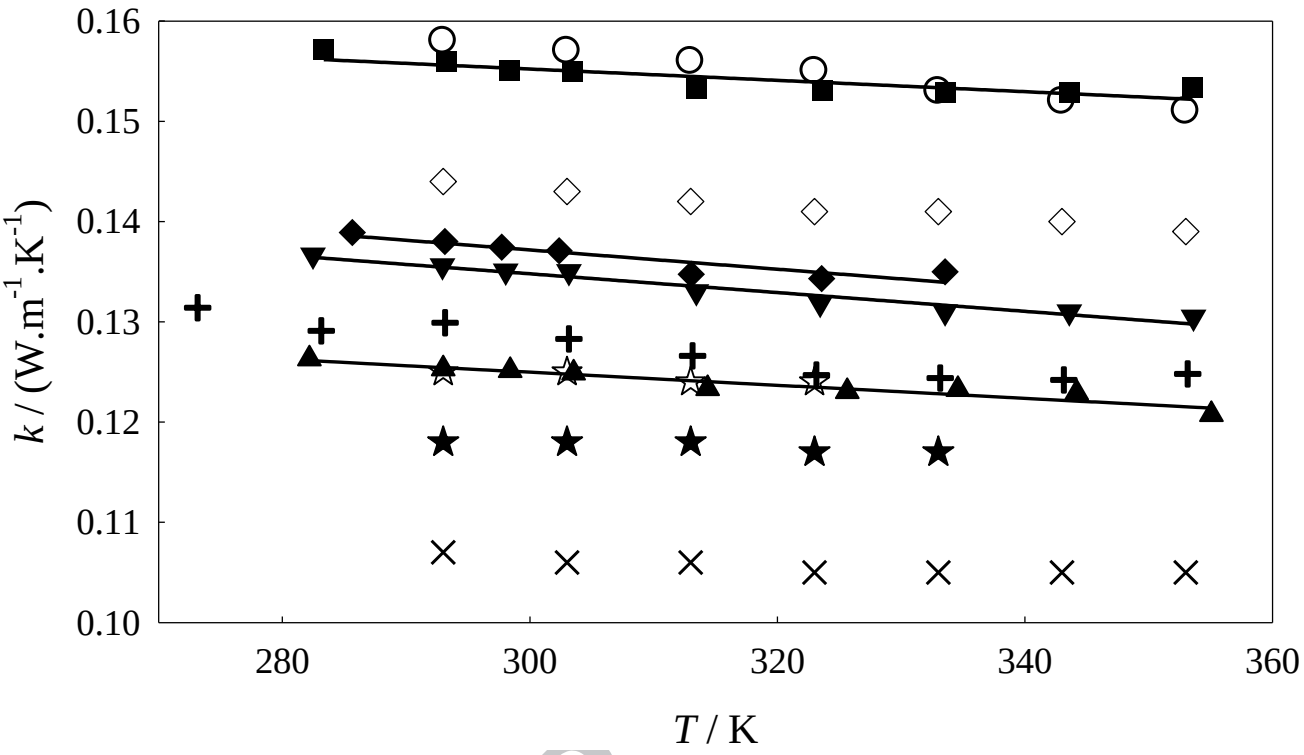

ACCEPTED

Ferreira *et al.* Figure 1

ACCEPTED MANUSCRIPT

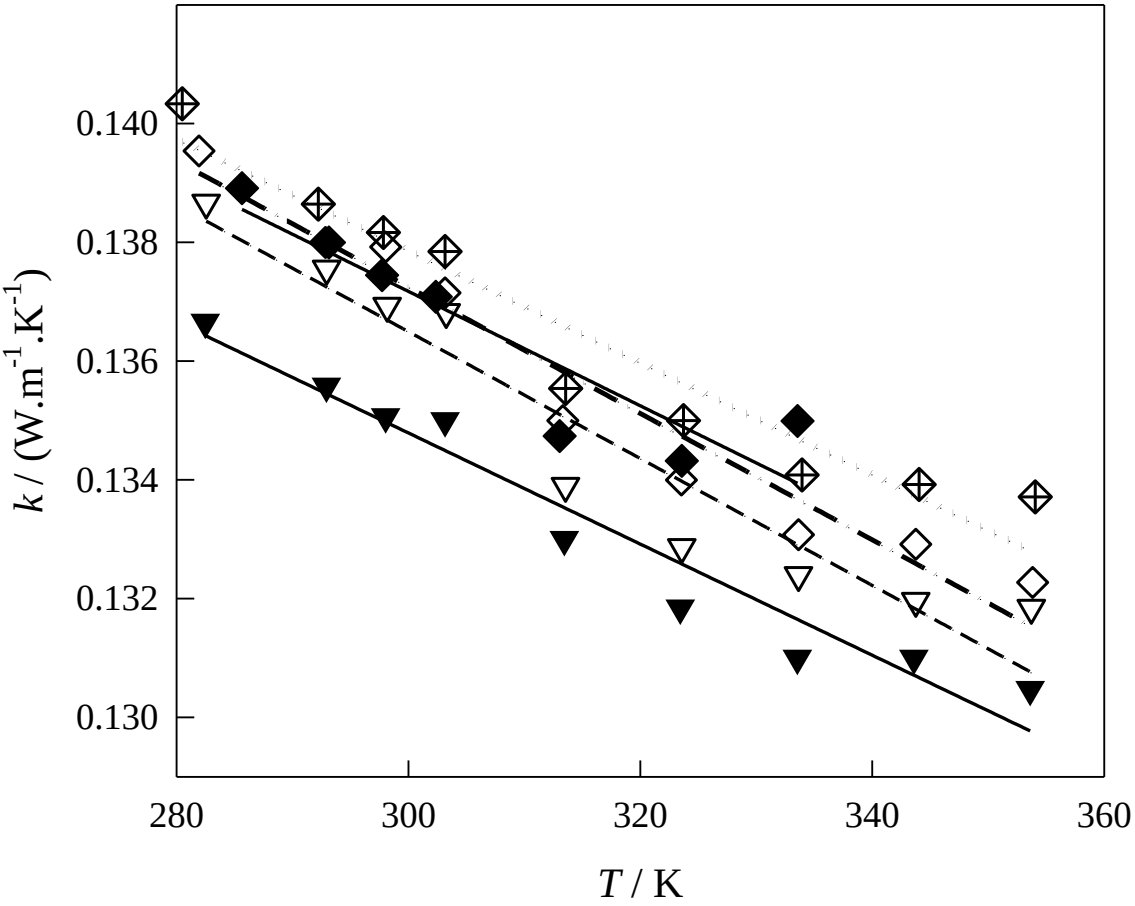

Ferreira *et al.* Figure 2

ACCEPTED MANUSCRIPT

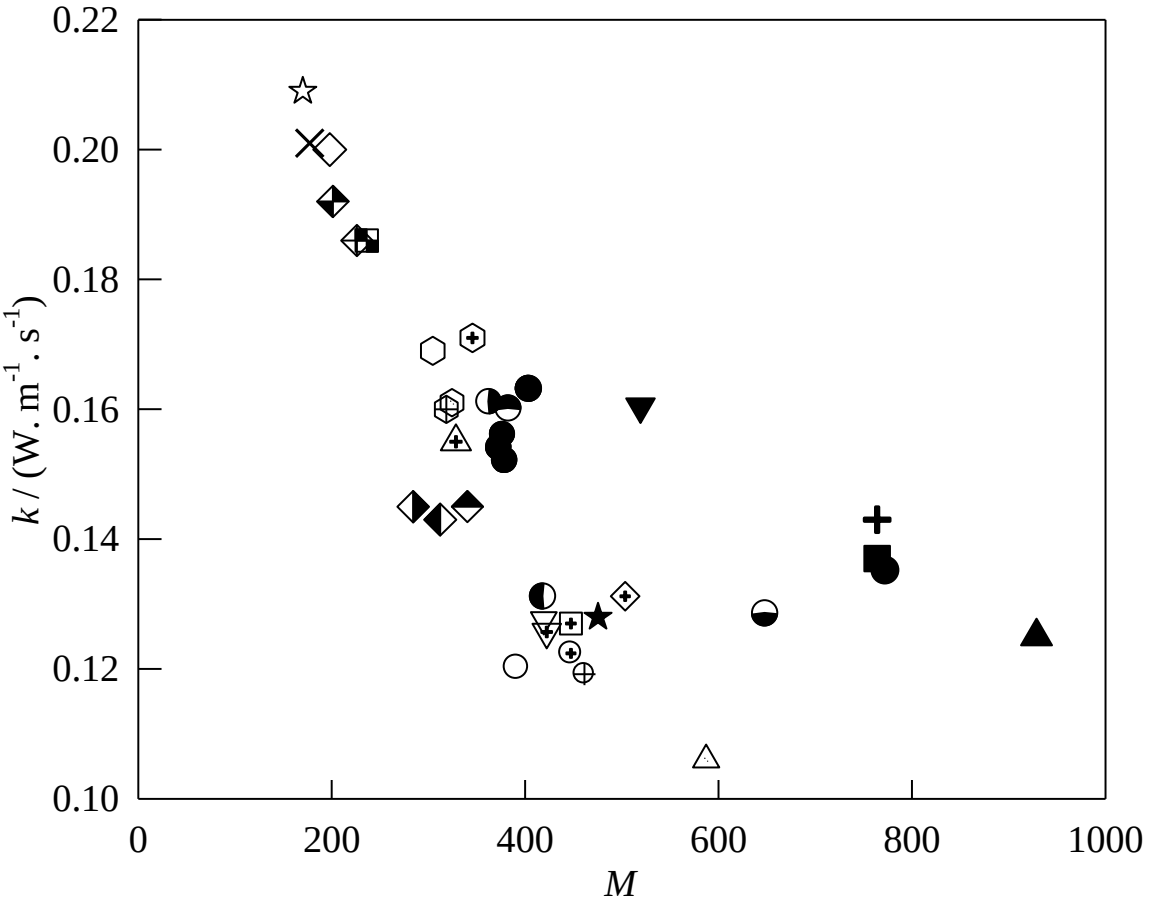

Ferreira *et al.* Figure 3

ACCEPTED MANUSCRIPT

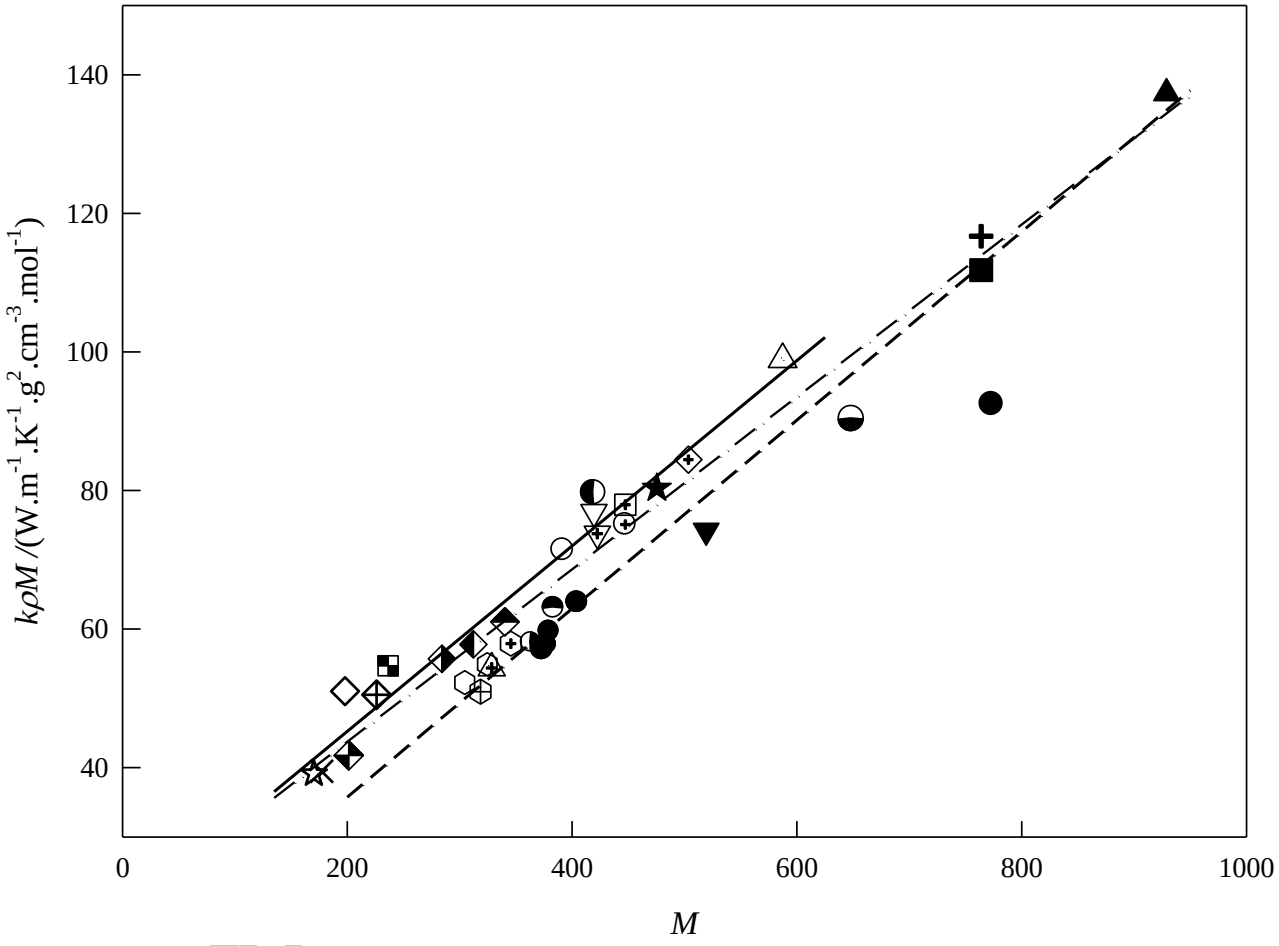

ACCE

Ferreira *et al.* Figure 4

ACCEPTED MANUSCRIPT

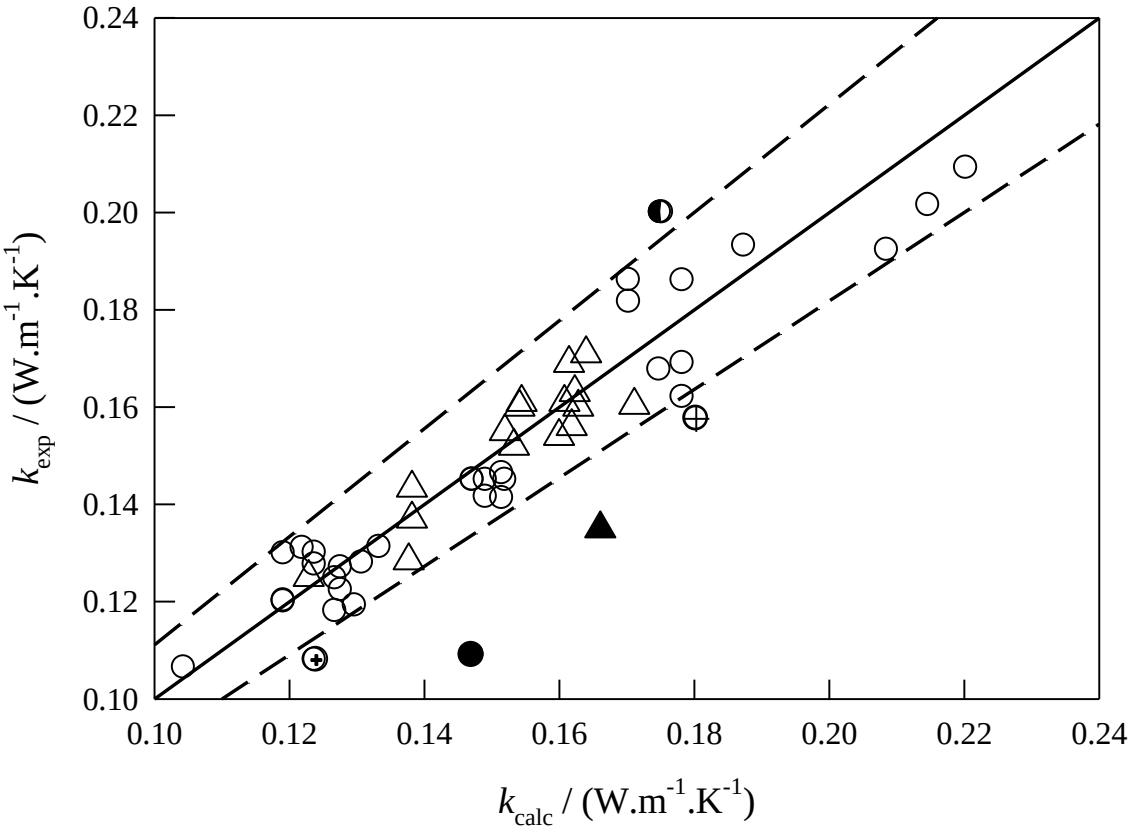

Ferreira *et al.* Figure 5

ACCEPTED MANUSCRIPT

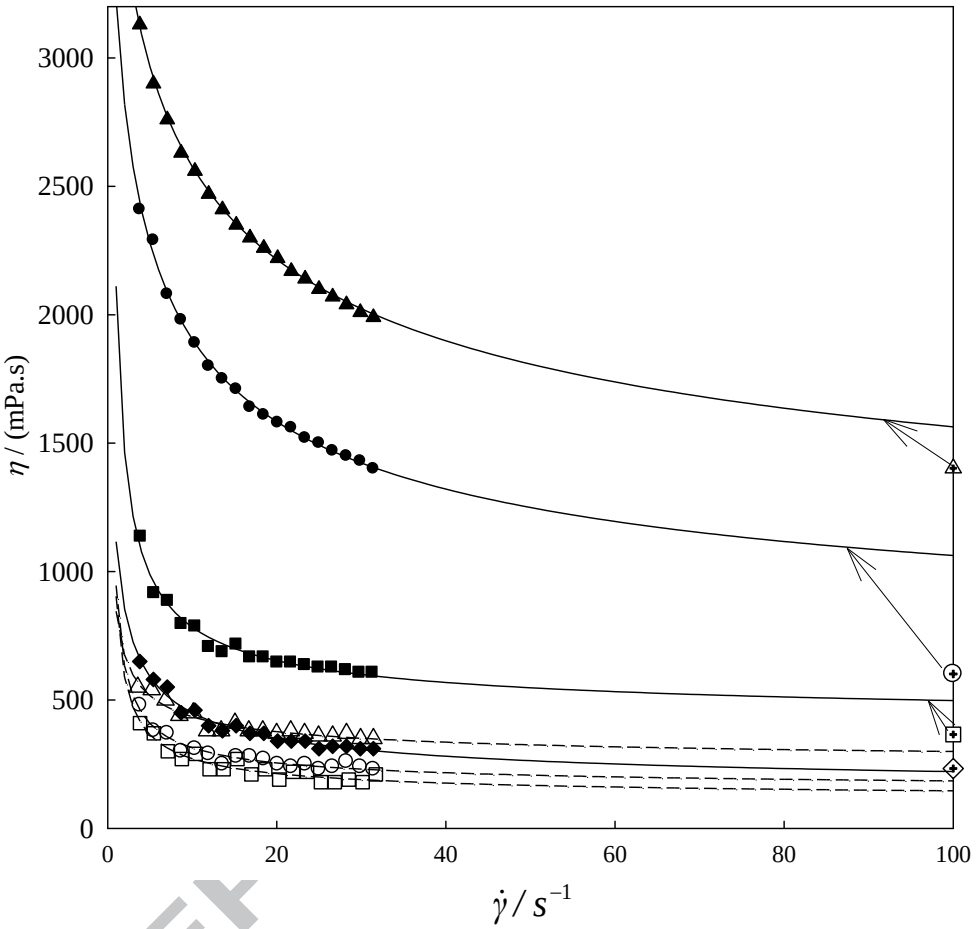

Ferreira *et al.* Figure 6

ACCEPTED MANUSCRIPT

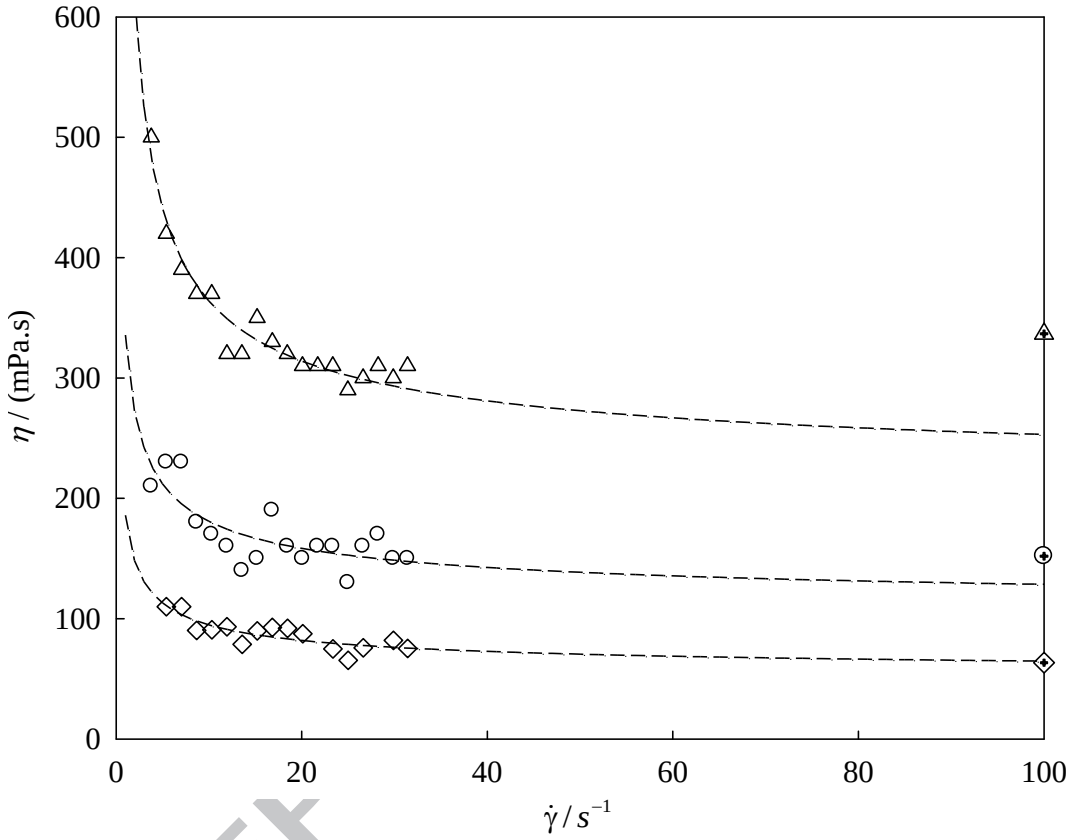

Ferreira *et al.* Figure 7

ACCEPTED MANUSCRIPT

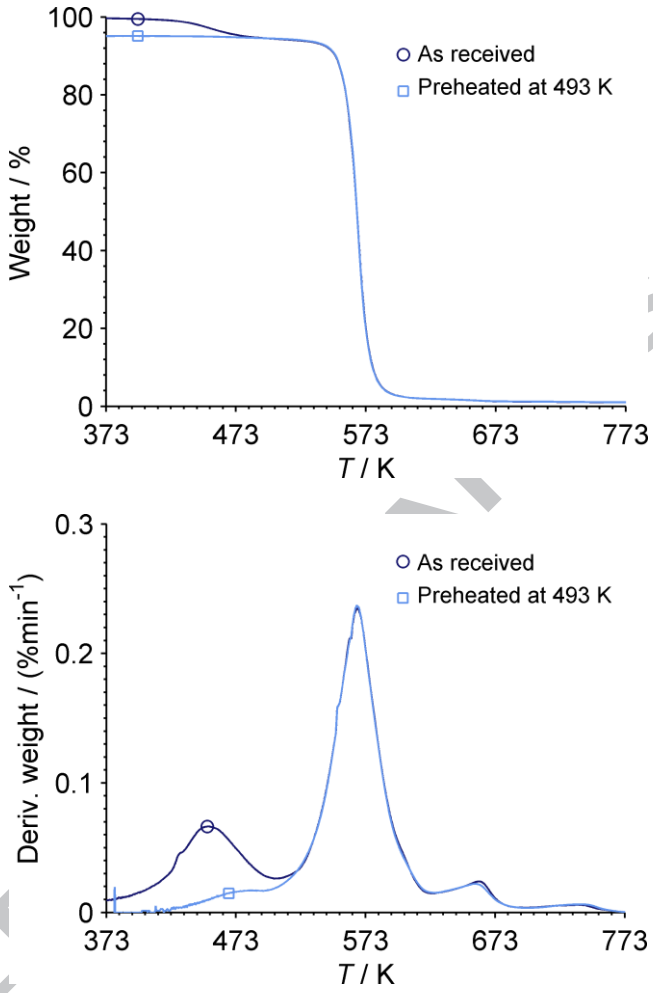

Ferreira *et al.* Figure 8

ACCEPTED MANUSCRIPT

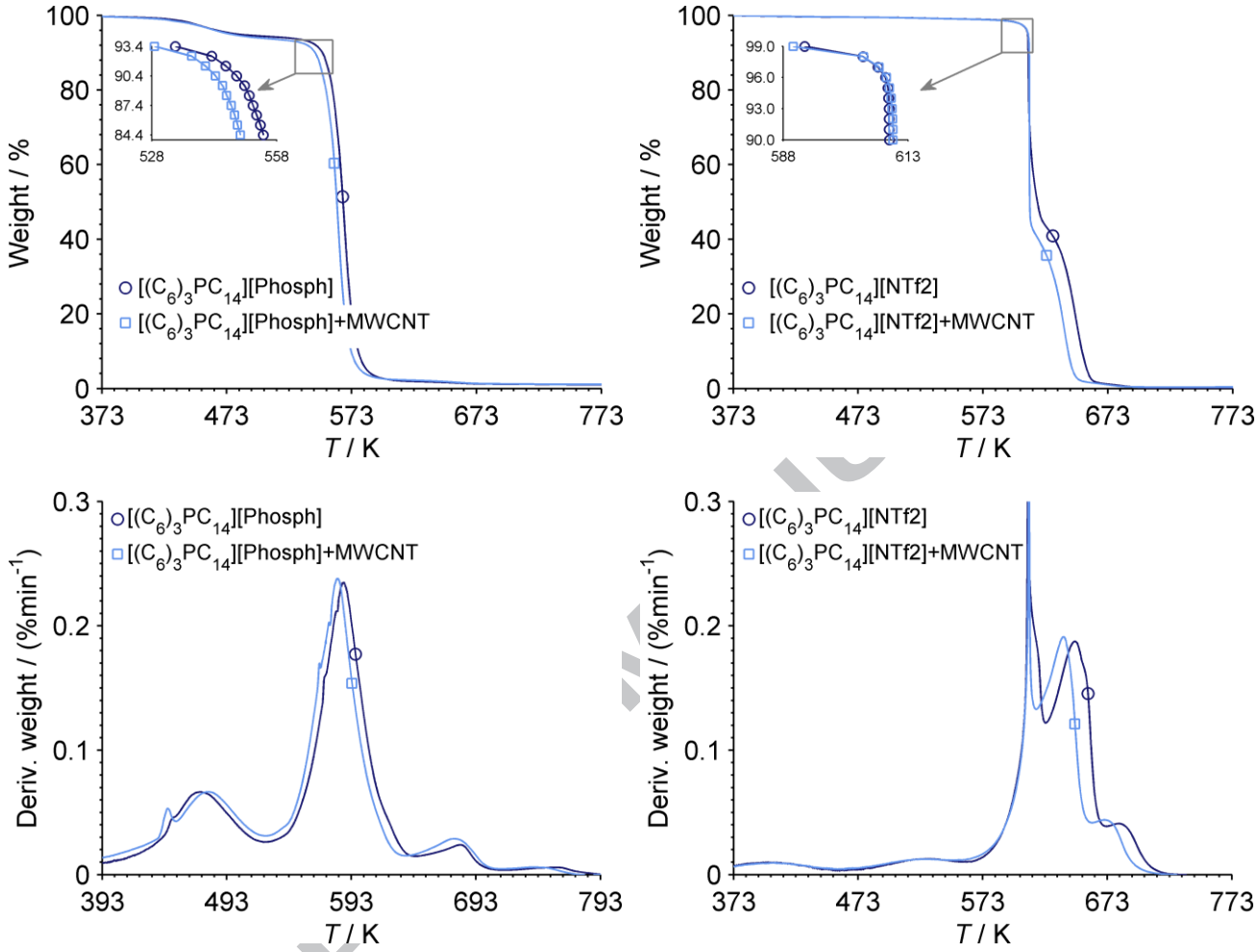

Ferreira *et al.* Figure 9

ACCEPTED MANUSCRIPT

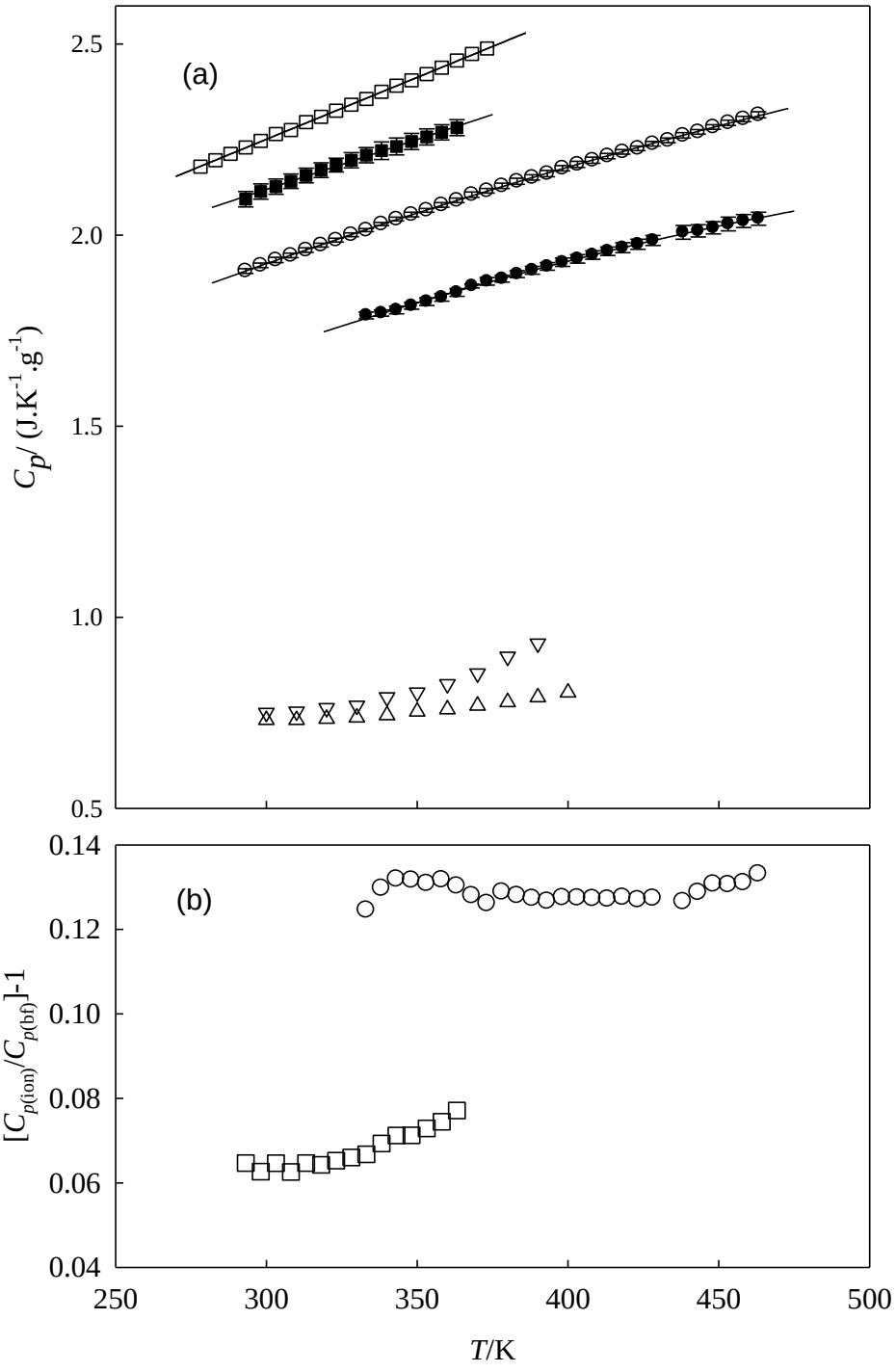

Ferreira *et al.* Figure 10

ACCEPTED MANUSCRIPT

TABLE 1
Provenance and purity of the Ionic Liquids studied.

IL	Supplier	Mass fraction purity	
		As received [a]	After drying/10^{-6} [b]
$[(C_6)_3PC_{14})][Phosph]$	CYTEC	95.0 (ttppo, 0.2-0.5w)	< 200
$[(C_4)_3PC_1)][C_1SO_4]$	CYTEC	98.6 (<0.052h)	< 200
$[(C_6)_3PC_{14})][NTf_2]$	CYTEC	98.6 (<0.003h)	< 200
$[(C_6)_3PC_{14})][FAP]$	Merck	99.4 (<0.01 h; <1w)	< 130

[a] As received from the supplier; ttppo, tris-2,4,4-trimethylpentylphosphine oxide; w, water; h, halides.
[b] Water content after drying under vacuum at *ca*. T = 343 K.

TABLE 2
Thermal conductivity (k) as function of temperature (T) of the studied quaternary phosphonium ILs and IoNanofluids obtained from MWCNT mixed with quaternary phosphonium ILs at p^o = 101.325 kPa.

$[(C_6)_3PC_{14})][FAP]$		$[(C_6)_3PC_{14})][Phosph]$		$[(C_6)_3PC_{14})][NTf_2]$		$[(C_4)_3PC_1)][C_1SO_4]$	
T/K	k/(W m^{-1} K^{-1})	T/K	k /(W m^{-1} K^{-1})	T/K	k/(W m^{-1} K^{-1})	T/K	k /(W m^{-1} K^{-1})
282.19	0.126	282.47	0.137	285.65	0.139	283.34	0.157
292.99	0.125	292.94	0.136	293.14	0.138	293.28	0.156
298.41	0.125	298.04	0.135	297.72	0.137	298.36	0.155
303.54	0.125	303.15	0.135	302.37	0.137	303.45	0.155
314.37	0.123	313.45	0.133	313.04	0.135	313.50	0.153
325.65	0.123	323.45	0.132	323.58	0.134	323.60	0.153
334.58	0.123	333.55	0.131	333.55	0.135	333.58	0.153
344.18	0.123	343.59	0.131			343.61	0.153
355.07	0.121	353.62	0.131			353.51	0.153

$[(C_6)_3PC_{14})][Phosph]$ +MWCNT (=0.05v/v%)		$[(C_6)_3PC_{14})][NTf_2]$ /MWCNT (=0.05v/v%)		$[(C_6)_3PC_{14})][NTf_2]$ /MWCNT (=0.1v/v%)	
282.57	0.139	281.95	0.140	280.49	0.140
292.95	0.138	292.85	0.138	292.24	0.139
298.17	0.137	298.03	0.138	297.85	0.138
303.25	0.137	303.17	0.137	303.15	0.138
313.55	0.134	313.31	0.135	313.56	0.136
323.58	0.133	323.54	0.134	323.73	0.135
333.64	0.132	333.64	0.133	333.95	0.134
343.75	0.132	343.75	0.133	344.04	0.134
353.72	0.132	353.82	0.132	354.06	0.134

The experimental uncertainty in the values of thermal conductivity is less than ± 0.01W m^{-1} K^{-1}.
The experimental uncertainty in the temperature is ± 0.01K.

ACCEPTED MANUSCRIPT

TABLE 3
Fitting parameters, k_0 and k_1, of equation (1) for the thermal conductivity of the studied ILs and IoNanofluids.

ILs and IoNanofluids	$k_0 \pm \sigma_{k0}$ /(W·m^{-1}·K^{-1})	$(k_1 \pm \sigma_{k1})10^4$/(W·m^{-1}·K^{-2})	σ[a]/ (W·m^{-1}·K^{-1})
$[(C_6)_3PC_{14})][FAP]$	0.1445 ± 0.0024	-0.651 ± 0.076	0.001
$[(C_6)_3PC_{14}][Phosph]$	0.1629 ± 0.0260	-0.934 ± 0.081	0.001
$[(C_6)_3PC_{14}][NTf_2]$	0.1661 ± 0.0031	-0.963 ± 0.184	0.001
$[(C_4)_3PC_1][C_1SO_4]$	0.1721 ± 0.0039	-0.564 ± 0.123	0.001
$[(C_6)_3PC_{14}][Phosph]$ +MWCNT (=0.05v/v%)	0.1685 ± 0.0038	-1.068 ± 0.120	0.001
$[(C_6)_3PC_{14}][NTf_2]$ +MWCNT (=0.05v/v%)	0.1692 ± 0.0028	-1.065 ± 0.090	0.001
$[(C_6)_3PC_{14}][NTf_2]$ +MWCNT (=0.1v/v%)	0.1661 ± 0.0031	-0.942 ± 0.097	0.001

[a] σ_{ki}: uncertainties of the fitting parameter k_i; σ: the standard deviation of the linear fitting.

ACCEPTED MANUSCRIPT

ACCEPTED MANUSCRIPT

TABLE 4
Molar mass (M) density (ρ) and thermal conductivity (k) at T=298.15 K for the ILs used in correlation development.

IL	M	ρ_{298} / (g·cm^{-3})	k_{298} /(W m^{-1} K^{-1})	($k\rho M$)/(W m^{-1} K^{-1} ·g^2 cm^{-3} mol^{-1})
$[C_2C_1im][NTf_2]$	391.31	1.5187[a]	0.120[b]	71.43
$[C_4C_1im][NTf_2]$	419.37	1.4368[c]	0.128[b]	76.89
$[C_6C_1im][NTf_2]$	447.42	1.3715[d]	0.122[b],0.127[e]	75.09,77.95
$[C_8C_1im][NTf_2]$	475.47	1.3202[f]	0.128[e]	80.34
$[C_{10}C_1im][NTf_2]$	503.53	1.2783[g]	0.131[e]	84.45
$[C_4C_4im][NTf_2]$	461.44	1.3400[h]	0.119[b]	73.70
$[C_3C_1C_1im][NTf_2]$	419.36	1.4578[i]	0.131[j]	79.63
$[C_4C_1Pyr][NTf_2]$	422.41	1.3997[k]	0.125[e]	73.76
$[C_4C_1Pyr][FAP]$	587.27	1.5828[l]	0.106[e]	98.90
$[C_2C_1im][BF_4]$	197.98	1.2958[m]	0.200[j]	51.03
$[C_4C_1im][BF_4]$	226.02	1.2087[n]	0.186[j]	50.52
$[C_4C_1im][PF_6]$	284.18	1.3603[o]	0.145[p]	56.11
$[C_6C_1im][PF_6]$	312.23	1.2939[q]	0.143[p]	57.77
$[C_8C_1im][PF_6]$	340.29	1.2371[r]	0.145[s]	61.04
$[C_2C_1im][OAc]$	170.21	1.0997[t]	0.209[t]	39.12
$[C_2C_1im][EtSO_4]$	236.30	1.2443[u]	0.186[t]	54.71
$[C_2C_1im][C(CN)_3]$	201.24	1.0814[t]	0.192[t]	41.78
$[C_2C_1im][N(CN)_2]$	177.20	1.1085[v]	0.201[t]	39.48
$[(C_8)_3NC_1)][NTf_2]$	648.90	1.0833[x]	0.1284[b]	90.25
$[(C_6)_3PC_{14})][Cl]$	519.31	0.8908[y]	0.160[e]	74.02
$[(C_6)_3PC_{14})][NTf_2]$	764.01	1.0652[w]	0.137[z],0.143[e]	111.81,116.69
$[(C_6)_3PC_{14})][Phosph]$	773.27	0.8853[a1]	0.135[z]	92.42
$[(C_6)_3PC_{14})][FAP]$	928.86	1.1818[a2]	0.125[z]	137.22
$[(C_4)_3PC_1)][C_1SO_4]$	328.45	1.0662[a3]	0.155[z]	54.28
$[(C_4)_3NC_1][Ser]$	304.47	1.016[a4]	0.169 [a4]	52.28
$[(C_4)_3NC_1][Tau]$	324.52	1.051 [a4]	0.161 [a4]	54.91
$[(C_4)_3NC_1][Lys]$	345.57	0.980 [a4]	0.171 [a4]	57.91
$[(C_4)_3NC_1][Thr]$	318.50	1.000 [a4]	0.160 [a4]	50.96
$[(C_4)_4P][Ser]$	363.53	0.992 [a4]	0.161 [a4]	58.06
$[(C_4)_3NC_1][Tau]$	383.59	1.027 [a4]	0.160 [a4]	63.03
$[(C_4)_3NC_1][Lys]$	404.63	0.968 [a4]	0.163 [a4]	63.84
$[(C_4)_3NC_1][Thr]$	377.56	0.980 [a4]	0.156 [a4]	57.72
$[(C_4)_3NC_1][Pro]$	373.57	0.993 [a4]	0.154 [a4]	57.13
$[(C_4)_3NC_1][Cys]$	379.60	1.034 [a4]	0.152 [a4]	59.66

[a] Calculated from equation (4) (ρ_0=0.6188,ρ_1= -6.739x10^{-4}, =0.001; Refs: [16],[17],[18],[19]); [b] Calculated from equation (1) given by Fröba *et al.*[3]. [c] From equation (4) (ρ_0=5308,ρ_1= -4.856x10^{-4}, =0.001; Refs: [15], [16],[17],[20],[21],[22]); [d] From equation (4) (ρ_0=0.4852,ρ_1= -4.9303x10^{-4}, =0.001; Refs: [15],[17],[23],[24]);[e] From equation (1) given by Ge *et al.*[4].. [f] From equation (4) (ρ_0=0.4590,ρ_1= -5.570x10^{-4}, =0.001; Refs: [15],[17],[18],[19]); [g] From equation (4) (ρ_0=0.4200,ρ_1= -5.1768x10^{-4}, =0.001;

ACCEPTED MANUSCRIPT

Refs: [15],[17],[19],[22],[25]); [h] From equation (4) (ρ_0=0.4935,ρ_1= -6.737 10^{-4}, =0.000; Refs: [26]). [i] Calculated from equation (4) (ρ_0=0.5512,ρ_1= -5.845x10^{-4}, =0.002; Refs: [27]); [j] Calculated from equation (1) given by Van Valkenburg *et al*.[1]. [k] Calculated from equation (4) (ρ_0=0.5374,ρ_1= -6.746 10^{-4}, =0.000; Refs: [28]). [l] From equation (4) (ρ_0=0.604,ρ_1= -6.748x10^{-4}, =0.000; Refs: [15]). [m] From equation (4) (ρ_0=0.6188,ρ_1= -6.739x10^{-4}, =0.001; Refs: [18],[29]). [n] From equation (4) (ρ_0=0.6188,ρ_1= -6.739x10^{-4}, =0.001; Refs: [15], [21], [30], [31], [32], [33], [34], [35], [36], [37],[38]). [o] Calculated from equation (4) (ρ_0=0.6188,ρ_1= -6.739x10^{-4}, =0.001; Ref: [35])); [p] Calculated from equation (1) with parameters obtained from values given by Tomida *et al*.[7] and Castro *et al*. [9]. [q] Calculated from equation (4) (ρ_0=0.4480,ρ_1= -6.383x10^{-4}, =0.000; Refs: [32])); [r] Calculated from equation (4) (ρ_0=0.4027,ρ_1= -6.370x10^{-4}, =0.00; Refs: [32]). [s] Calculated from equation (1) with parameters obtained from values given by Tomida *et al*.[7]. [t] Densities from equation $\rho = \rho_0+\rho_1 T+\rho_0 T^2$ with (ρ_0=1.305, ρ_1= -7.6268x10^{-4}, ρ_2=2.4838x10^{-7}, =0.004) and k from equation (1) both given by Fröba *et al*.[3]). [u] Value given by Luciana *et al.* [25]). [v] Densities from equation (4) (ρ_0=0.2776, ρ_1= -5.857x10^{-4}, =0.001); Ref [40]). [x] Densities from equation (4) (ρ_0=0.2527,ρ_1= -5.791x10^{-4}, =0.001); Ref [41]). [y] Densities from equation (4) (ρ_0=0.08703, ρ_1= -6.796x10^{-4}, =0.001); Refs [42],[43],[44]). [w] Densities from equation (4) (ρ_0=0.1929, ρ_1= -2.060 10^{-4}, ρ_2=-7.680x10^{-7}, =0.001); Refs [15],[19],[44]). [z] From table 1. [a1] Densities from equation (4) (ρ_0=0.0787,ρ_1= -6.726x10^{-4}, =0.000); Refs [43]). [a2] Densities from equation (4) (ρ_0=0.3676,ρ_1= -6.726x10^{-4}, =0.00); Refs [45]). [a3] Refs [46]).]). [a4] Value given By Gardas *et al.* [5]).

ACCEPTED MANUSCRIPT

ACCEPTED MANUSCRIPT

TABLE 5

Fitting parameters of equation (15) for the (η, $\dot{\gamma}$) data for $[(C_6)_3PC_{14}][Phosph]$ IL and IoNanofluids.

T/K	η /mPa.s	τ_0/mPa	/s^{-1}	σ^a/(mPa.s)
		$[(C_6)_3PC_{14}][Phosph]$		
298.15	847.30	$1.895\ 10^4$	10.206	9
313.15	568.54	$1.151\ 10^4$	5.078	19
323.15	387.46	689.81	$1.66\ 10^{-9}$	23
333.15	125.61	$1.555\ 10^3$	0.602	23
		$[(C_6)_3PC_{14}][Phosph]$+0.05 v % MWCNT		
298.15	238.36	374.38	0.175	18
313.15	136.50	363.64	$7.21\ 10^{-9}$	17
323.15	100.90	417.10	$4.16\ 10^{-4}$	20
		$[(C_6)_3PC_{14}][NTf_2]$+0.1 v% MWCNT		
298.15	208.40	215.89	$2.79\ 10^{-10}$	14
313.15	104.56	133.59	0.183	19
333.15	51.214	85.73	0.184	20

[a] : standard deviation of the fittings.

ACCEPTED MANUSCRIPT

ACCEPTED MANUSCRIPT

TABLE 6
Characteristic quantities obtained from HRMTGA curves (2 K·min^{-1}; amplitude of modulation: ± 5ºC; period of modulation 200 s). T_{on}: extrapolated onset temperature; T_p: peak temperature(s) (DTG curves) corresponding to the main mass loss stage; m_r: residual mass at T = 873 K.

Sample	T_{on}/K	T_p/K		m_r/%
$[(C_6)_3PC_{14})][Phosph]$ as received	557.4	567.3		1.03
$[(C_6)_3PC_{14})][Phosph]$ preheated at 493 K	557.7	567.8		1.05
$[(C_6)_3PC_{14})][Phosph]$+MWCNT	553.5	562.3		1.11
$[(C_6)_3PC_{14}][NTf_2]$	612.3	612.8	649.5	0.26
$[(C_6)_3PC_{14}][NTf_2]$+MWCNT	610.2	610.3	639.9	0.43

ACCEPTED MANUSCRIPT

ACCEPTED MANUSCRIPT

TABLE 7
Fit parameters of equation (16) for the heat capacity as function of temperature of the ILs and IoNanofluids studied.

ILs and IoNanofluids	c_0/(J·K^{-1}·g^{-1})	$c_1 10^3$/(J·K^{-2}·g^{-1})	$c_2 10^6$/(J·K^{-3}·g^{-1})	σ^a/(J·K^{-1}·g^{-1})
[$(C_6)_3PC_{14}$)][Phosph]	1.335	2.615	0	0.003
[$(C_6)_3PC_{14}$][NTf_2]	0.582	4.743	-3.421	0.003
[$(C_6)_3PC_{14}$][Phosph] +0.05 v% MWCNT	1.279	3.239	0	0.002
[$(C_6)_3PC_{14}$][NTf_2] +0.1 v% MWCNT	0.872	4.248	-2.458	0.002

[a] : standard deviation of the fitting.

ACCEPTED MANUSCRIPT

ACCEPTED MANUSCRIPT

Research Highlights

► Phosphonium Ionic Liquids (ILs) and multiwalled carbon nanotubes (MWCNT) suspensions (IoNanofluids).

► Transport (thermal conductivity, viscosity) and thermal properties (thermal stability, heat capacity).

► Hot-wire method. Controlled stress rheometry. High resolution modulated TGA. Modulated-DSC.

► Predictive models for thermal conductivity of ILs based on extensive experimental data.

► Enhancement of thermophysical and transport properties of phosphonium ILs and MWCNT based IoNanofluids.

ACCEPTED MANUSCRIPT